

This is the peer-reviewed version of the following article:

Erceg, T., Vukić, N., Šovljanski, O., Stupar, A., Šergelj, V., Aćimović, M., Baloš, S., Ugarković, J., Šuput, D., Popović, S., Rakić, S. (2022). Characterization of films based on cellulose acetate/poly(caprolactone diol) intended for active packaging prepared by green chemistry principles. *ACS Sustainable Chemistry & Engineering*, published online on 7 July 2022.

This document is the Accepted Manuscript version of a Published Work that appeared in final form in *ACS Sustainable Chemistry & Engineering*, copyright © American Chemical Society after peer review and technical editing by the publisher. To access the final edited and published work see <https://doi.org/10.1021/acssuschemeng.2c02009>.



This work is **licensed** under

Creative Commons - Attribution-Noncommercial-NoDerivative Works 4.0 International

**Characterization of films based on cellulose  
acetate/poly(caprolactone diol) intended for active packaging  
prepared by *green* chemistry principles**

Tamara Erceg 1†\*, Nevena Vukić 2‡, Olja Šovljanski 1†, Alena Stupar 3†,‡, Vanja Šergelj 1†,  
Milica Aćimović 1†, Sebastian Baloš 4‡‡, Jovana Ugarković 1†, Danijela Šuput 1†, Senka  
Popović 1†, Srđan Rakić 5 †‡‡

1† University of Novi Sad, Faculty of Technology Novi Sad, Bulevar cara Lazara 1, 21000 Novi  
Sad, Serbia

2‡ University of Novi Sad, University of Kragujevac, Faculty of Technical Sciences, Svetog  
Save 65, 32000 Čačak, Serbia

3†,‡ University of Novi Sad, Institute of Food Technology in Novi Sad, Bulevar cara Lazara 1,  
21000 Novi Sad, Serbia

4‡‡ University of Novi Sad, Faculty of Technical Sciences, Trg Dositeja Obradovića 6, 21000  
Novi Sad, Serbia

5 †‡‡ University of Novi Sad, Faculty of Sciences, Trg Dositeja Obradovića 3, 21000 Novi Sad,  
Serbia

Corresponding author: Tamara Erceg\*

tamara.erceg@uns.ac.rs

## **Abstract**

Biodegradable active packaging films based on cellulose acetate and poly(caprolactone diol) blend with incorporated lemongrass oil were developed. Films were prepared using the novel bio-based, plasticizer glycerol tritartarate, synthesized using the principles of *green* chemistry. The influence of plasticizer, as well as essential oil amount on the structural, surface, mechanical and thermal properties of blends, was investigated. Plasticizer has been displayed as a compatibilizer for two polymers, according to the results of SEM and surface energy analysis. Blends with a greater amount of plasticizer possess better mechanical properties, but worse resistance to water. The antimicrobial properties of blends with lemongrass oil were found to be superior to blends without essential oil. The incorporation of lemongrass oil in polymer blend has resulted in one more step longer thermal degradation process. Optimal films properties, biodegradability, cost-effective

preparation method, and additional functions make these films suitable for the production of packaging for grapefruit.

**KEYWORDS:** *Cellulose acetate, Poly(caprolactone diol), glycerol tritartarate, lemongrass oil, blends, biodegradable active packaging, torsion resistance*

## **Introduction**

The packaging industry is the largest and fastest-growing consumer of synthetic conventional plastic materials, which is highly dependent on fossil resources. Also, this industry, especially single-use plastics intended for food and beverages, is the main source of supplying waste plastics into the environment at an alarming rate creating a problem of microplastics, as polymers do not degrade, but break down into smaller pieces, ending up in the air, soil, water as well as in living organisms.<sup>1-3</sup> This has created a need for the development of *green*, abundant, and economic alternatives to petrochemical plastic packaging materials such as bioplastic. The bioplastics industry is reported to be a young, innovative sector possessing great ecological and economic potential for a low-carbon, circular economy that utilizes resources more efficiently.<sup>4</sup> The main functions of food packaging have been the same throughout history: hygiene and protection during transportation and storing. Modern technology and materials have introduced new functionalities to packaging because the selection and development of packaging materials can be a partial solution to the complex problems of food safety and reduce unnecessary food waste.<sup>5</sup> Many terms are used to describe packaging with new functions, and one of them is active packaging, which involves the use of polymers that act as supports for various active compounds that can be incorporated during the packaging manufacturing process.<sup>6, 7</sup> Active packaging provides extraordinary as well as vital functions to food products with an extended shelf life, while ensuring their quality, safety, and integrity.<sup>8,9</sup> Active *green* food packaging will be one answer to the global challenges related to the desperate quest for carbon neutrality, food safety, and food saving, as well as renewable materials and technologies.<sup>5</sup> Sustainable active packaging materials should be tailored to impose a lower impact on the health of consumers as well as the environment. Food packaging materials can be enriched with antimicrobials, which affect the growth of pathogens in food. Active agents slowly release from the packaging material and dissolve onto the surface of the food through direct contact, with the aim of extending the shelf life and organoleptic properties of the food product.<sup>10</sup> Huge amounts of food spoiled by microbial contamination represent one of

the essential problems in food distribution and storage processing. For example, fungi are responsible for the loss of about 20% of the yield of fruits and vegetables globally, which is enough food to feed millions of people. It is estimated that at least 125 million tons of fruits and vegetables are manually contaminated in Europe, with an increasing trend every year, which indicates the importance of this problem.<sup>11</sup> Natural compounds obtained from plants represents an alternative and eco-based replacement for antibiotics since there do not contribute to antimicrobial resistance, are needed in small quantities and are obtained from different type of waste.<sup>12</sup> Essential oils, with recognized antimicrobial properties, can be used for this purpose as natural additives in packaging applications.<sup>13</sup>

Cellulose derivatives are usually most relevant for packages that come into direct contact with food. Cellulose acetate (CA) is a low-cost thermoplastic biopolymer widely used for primary food packaging applications as a rigid wrapping film, and it has some inherent drawbacks. To counter its drawbacks, blending cellulose acetate with other biopolymers can be a solution for environmentally friendly, low-cost packaging materials with improved properties. In order to improve mechanical properties and processability, cellulose acetate has been blended with biodegradable poly(caprolactone) (PCL) which has been used as a route to make processable food packaging material. There are several reports in which CA is blended with PCL by dissolving polymers in acetone without and with compatibilizer (polyethylene-graft-glycidyl methacrylate).<sup>14</sup> The obtained results have showed an improvement in the mechanical and thermal properties of blends after the addition of a compatibilizer. Naggar et al. have synthesized an eco-friendly antimicrobial film based on cellulose acetate and poly(caprolactone) loaded with copper nanoparticles for food packaging applications. The produced films have displayed good mechanical properties and excellent air permeability when compared with films formed without copper nanoparticles.<sup>15</sup> In a number of studies, PCL-based fibers were electrospun with CA fibers to improve wetting properties and broaden the field of application, such as in biomedicine. A group of authors has prepared microfibers from CA blended with PCL loaded with different essential oils for potential application in biomedical fields. The initial idea for the combination of CA with PCL was to improve CA processing properties, flexibility, and durability. A group of authors has prepared microfibers from CA blended with PCL loaded with different essential oils for potential application in biomedical fields. The initial idea for the combination of CA with PCL was to improve CA processing properties, flexibility, and durability. With the same intention, CA has

been mixed with another polymer with plasticizing effects, such as poly(ethylene glycol)<sup>16</sup>, poly(ethylene succinate),<sup>17</sup> poly(vinyl acetate),<sup>18</sup> poly(N-vinyl pyrrolidone),<sup>19</sup> polyaniline,<sup>20</sup> etc. Different authors have investigated the plasticizing effect of low molecular weight substances such as biocompatible triacetin, tripropionin, triethyl citrate, tributyl citrate, and tributyl 2-acetyl citrate<sup>21</sup> as a substitute for toxic phthalates. Meier and co-authors have investigated the structural, thermal, and mechanical properties of CA films plasticized with different amounts (up to 50 wt%) of low molecular weight poly(caprolactontriol).<sup>22</sup> However, researching the available literature, it has not been found a study about biodegradable polymer films based on CA and polyester poly(caprolactone diol) (PCL-diol) plasticized with fully bio-based, cost-effective plasticizer prepared from glycerol and tartaric acid – glycerol tritartarate (GTT), which also proved to be a good compatibilizing agent, improving the mixing of polymers in the blend. In our view, it should be possible to obtain films based on CA, PCL-diol, and GTT using a cost-effective, solution-casting method, intended for active packaging in the food industry.

Therefore, the aim of this study was to prepare CA/PCL-diol blends with different amounts of GTT and active packaging based on the obtained material using a pure lemongrass essential oil as an antimicrobial agent. The initial idea for blending CA with PCL-diol was to achieve brittleness reduction of CA, starting from the premise of good miscibility of these polymers considering their solubility in acetone and the presence of hydroxyl groups in their structure. CA exposes better miscibility with PCL-diol than with PCL; the formation of films with good properties based on CA and PCL is not possible without a compatibilizer, which has been confirmed by available literature and preliminary testing. Preliminary testing was also performed using a neat CA with a different amount of synthesized plasticizer, but the mechanical and barrier properties of obtained films were not satisfying. Obtained blends prepared in a *green* chemistry framework were thoroughly studied in terms of their structural, mechanical, thermal, and barrier properties and applied for packaging for grapefruits, considering the susceptibility of this fruit to fungi. A novel plasticizer has also demonstrated the function of a compatibilizer. In this study, the method for the determination of the angle of torsion is applied for the first time in order to investigate the mechanical properties of films during twisting, which is a frequent deformation of packaging during manipulation.

## Experimental Section

### Materials

Cellulose acetate ( $M_n \sim 50000$  g/mol, average acetyl content of 39.7 wt.%), poly(caprolactone diol) ( $M_n \sim 2000$  g/mol) (Figure 1), tartaric acid (TA) were purchased from Sigma Aldrich (USA). Acetone (pro analysis) and sulphuric acid (pro analysis), glycerol and dimethyl sulfoxide (DMSO) were supplied from ZORKA Pharma (Serbia).

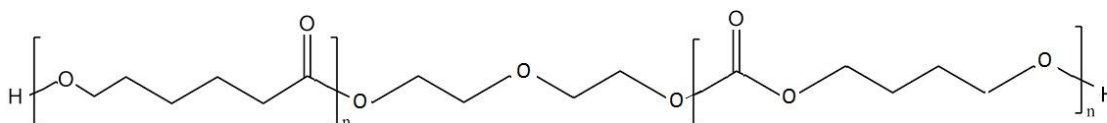


**Figure 1.** A chemical structure of PCL-diols.

### Preparation of plasticizer/compatibilizer

The plasticizer was prepared by the esterification reaction between glycerol and tartaric acid in a molar ratio 1:3. In order to gain a great yield of triglyceride, tartaric acid was added in three steps to glycerol. After the dissolution of tartaric acid in a minimum amount of water, one-third of the solution mass was added to the preweighed total mass of glycerol. The reaction of esterification between tartaric acid and glycerol was taken place for 120 min at 110 °C, while the second and third thirds of the tartaric acid solution mass were added over 80 minutes. Sulfuric acid was used as a catalyst (3 drops). The chemical structure of the plasticizer has given in Figure 2.

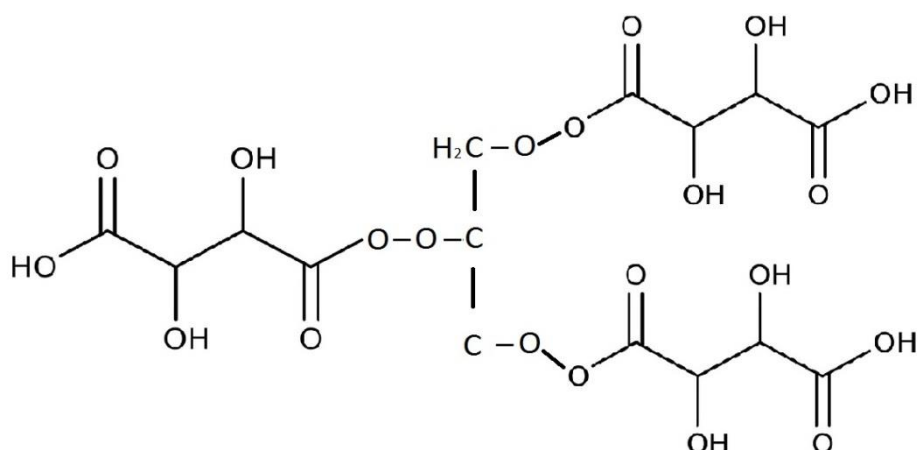


**Figure 2.** A chemical structure of plasticizer GTT.

### Preparation of Lemongrass oil

Lemongrass (*Cymbopogon citratus*) was grown at a greenhouse located in the village Banatska Topola (45°40'N; 20°27'E; altitude 78 m). Aboveground parts were harvested in July, dried in shade, and subjected to steam distillation. Briefly, 100 kg of dry plant material was placed in a distillation vessel ( $V = 0.8 \text{ m}^3$ ), routed upwards through a plumbing system, and supplied with steam. After 20 min the condensed vapor has started to collect in the Florentine flask. After 3 h the distillation process was over. The accumulated essential oil was decanted from the water phase, dried over sodium sulfate, and stored in amber glass bottles at 4 C° until further analysis. The main compounds of lemongrass oil are neral, citral, nonan-4-ol, camphene, 6-metil-hept-5-en-2-one, citronellal,  $\beta$ -caryophyllene, citronellol, caryophyllene oxide,  $\gamma$ -murolene, limonene, geranyl acetate, and geranial.<sup>23</sup>

### Preparation of CA/PCL-diol blends

Blends were prepared by solution blending of CA and PCL-diol in a weight ratio of 1:1. After the dissolution of cellulose acetate (8 wt%) in acetone, PCL-diol was added to the solution. The mixture was homogenized at 45 °C for two hours at a magnetic stirrer (1200 rpm), with and without the addition of plasticizer/compatibilizer, which was added in different amounts per total polymers

weight (Table 1), to investigate its influence on compatibilization of polymers, as well as structural, mechanical, and applicative properties of obtained blends. One series of samples with the same amount of plasticizer/compatibilizer was prepared by variation of lemongrass oil amount in order to get films for active packaging with an optimized composition that demonstrates antimicrobial and antioxidant properties. After homogenization of CA, PCL-diol, and plasticizer/compatibilizer in acetone, lemongrass oil was added in an amount of 3, 5, and 7 wt% (counted on the total mass of polymers in a blend). Solution - casting method was employed for the preparation of films.

**Table 1.** Composition of polymer blends.

Sample	Amount of GTT (wt%)
CA/PCL- diol 0% <sup>a</sup>	0
CA/PCL – diol 5% <sup>b</sup>	5
CA/PCL - diol 7% <sup>c</sup>	7
CA/PCL – diol 10% <sup>d</sup> -control	10
CA/PCL-diol 10% <sup>e</sup> 3% LG	
CA/PCL - diol 10% <sup>f</sup> , 5% LG	
CA/PCL-diol 10% <sup>g</sup> , 7% LG	
CA/PCL - diol 12% <sup>h</sup>	12

<sup>a</sup> Blend with weight CA/PCL-dol weight ratio of 1:1 without plasticizer/compatibilizer

<sup>b</sup> Blend with weight CA/PCL-dol weight ratio of 1:1 with 5 wt% of plasticizer/compatibilizer (per blend weight)

<sup>c</sup> Blend with weight CA/PCL-dol weight ratio of 1:1 with 7 wt% of plasticizer/compatibilizer (per blend weight)

<sup>d</sup> Blend with weight CA/PCL-dol weight ratio of 1:1 with 10 wt% of plasticizer/compatibilizer (per blend weight)

<sup>e</sup> Blend with weight CA/PCL-dol weight ratio of 1:1 with 10 wt% of plasticizer/compatibilizer (per blend weight), and 3 wt% of lemongrass oil (per polymer blend weight)

<sup>f</sup> Blend with weight CA/PCL-dol weight ratio of 1:1 with 10 wt% of plasticizer/compatibilizer (per blend weight), and 5 wt% of lemongrass oil (per polymer blend weight)

<sup>g</sup> Blend with weight CA/PCL-dol weight ratio of 1:1 with 10 wt% of plasticizer/compatibilizer (per blend weight), and 7 wt% of lemongrass oil (per blend weight)

<sup>h</sup> Blend with weight CA/PCL-dol weight ratio of 1:1 with 12 wt% of plasticizer/compatibilizer (per blend weight)

## FTIR analysis

The chemical structure of blends and a plasticizer was analyzed by Fourier-transform infrared spectroscopy (FTIR) (Thermo Fisher Scientific, MA, USA) operating in total reflectance attenuation (ATR) mode. All spectra were recorded in the spectral range 4000-400 cm<sup>-1</sup>, at a resolution of 4 cm<sup>-1</sup>.



### Scanning electron microscopy (SEM) analysis

The microstructure of polymer blends was investigated using the scanning electron microscope (JEOL JSM-6460, Japan) with an accelerating voltage of 20 kV. Samples were immersed in liquid nitrogen, cut, gold-sputter coated, and investigated under the different magnifications using the SCD-005 (Bal-tec/Leica, Wetzlar, Germany) device.

### Surface properties analysis

The surface energy of the films was investigated using contact angle experiments, performed by the sessile drop method, using two liquids (water and glycerol) at room temperature ( $24 \pm 1$  °C), according to the ISO 15989 standard.<sup>24</sup> After the deposition of the tested liquid on the film surface, the contact angle was determined by the analysis of an image using the Drop Shape Analyzer KRÜSS DSA25. The results of contact angle were reported as the average value of five measurements for each sample. The surface energy of each sample can be calculated using the following equations proposed by Owens and Wendt:<sup>25</sup>

$$\gamma_{L1} \frac{1 + \cos\theta_1}{2} = (\gamma_{L1}^d \cdot \gamma_s^d)^{\frac{1}{2}} + (\gamma_{L1}^p \cdot \gamma_s^p)^{\frac{1}{2}} \quad (1)$$

$$\gamma_{L2} \frac{1 + \cos\theta_2}{2} = (\gamma_{L2}^d \cdot \gamma_s^d)^{\frac{1}{2}} + (\gamma_{L2}^p \cdot \gamma_s^p)^{\frac{1}{2}} \quad (2)$$

$$\gamma_s^p + \gamma_s^d = \gamma_s \quad (3)$$

where  $\theta$  is the contact angle between film and liquid drop;  $\gamma_s$  is the surface energy of polymer films,  $\gamma_L$  surface energy of testing liquid, which represents the sum of surface energy due to dispersive interactions ( $\gamma_s^d, \gamma_L^d$ ) and surface energy due to polar interactions ( $\gamma_s^p, \gamma_L^p$ ). Distilled water was used as a testing liquid 1, whose corresponding dispersion and polarity compound values are 21.8, 51 mNm<sup>-1</sup>; glycerol was used as a testing liquid 2, whose surface energy value due to dispersive interactions is 37 mNm<sup>-1</sup>, and surface energy value which comes from polar interactions is 26.4 mNm<sup>-1</sup>.

### Moisture content and total soluble matter analysis

For determination of moisture content (MC) and total soluble matter (TSM), film samples were cut into square shapes with dimensions 20 x 20 mm, weighted and dried at  $105 \pm 2$  °C until they

reached a constant weight. The values of moisture content for each sample were calculated using the following Equation 4:<sup>26</sup>

$$MC = \frac{m_0 - m}{m_0} \cdot 100\% \quad (4)$$

where  $m_0$  is the initial mass of the film sample, and  $m$  is the mass of the sample after drying until the constant weight. The testing was carried out in three independent measurements, using the two samples, and the results were reported as an average value. In order to determine the solubility of samples, after drying until the constant weight at  $105 \pm 2$  °C, the specimens were weighted ( $m'$ ), put in 50 ml of distilled water and kept at room temperature for 24 h, with periodic stirring. After 24 h, the samples were taken out, dried at  $105 \pm 2$  °C until a constant weight and measured mass was recorded as a  $m''$ . TSM was calculated using the following Equation 5:

$$TSM = \frac{m' - m''}{m'} \cdot 100\% \quad (5)$$

### **Barrier properties - water vapour transmission rate**

The water vapour transmission rate (WVTR) for polymer films was determined according to the ISO standard,<sup>27</sup> which proposes a temperature of  $25 \pm 1$  °C and a relative humidity of  $90 \pm 2$  %. The results were averaged on three independent measurements.

### **Thickness**

The film thickness was measured by a micrometer (Digico 1, Tesa, Swiss Made, Renens, Switzerland), with a sensitivity of 0.001 mm, at 9 positions on two films from each sample, and the results were reported as the average value. The prepared films with obtained average thickness were used for the packaging formation.

### **Mechanical properties**

Tensile strength and elongation at break of polymer blends were investigated using the Instron Universal Testing Instrument Model 4301 (Instron Engineering Corp., Canton, MA) The samples were prepared and tested according to the ASTM standard D882-18, which implies a rectangular shape of specimens with 80 mm in nominal length and 15 mm in width. All tests were carried out at a temperature of  $23 \pm 2$  °C, with the initial grip separation set at 50 mm and the crosshead speed

set at 50 mm/min. Results were averaged on four independent measurements, and the extreme values were excluded.

To determine the prepared materials torsion resistance, a novel torsion angle testing was devised. It was performed on a standard tensile testing machine, where the 60 x 20 x 0.17 mm specimens were clamped in the fixed top grip (Figure 3). The other side of the specimen was clamped in the bottom grip, which had the weight of 1.5 kg, which was left loose in terms of torsion. Its bottom part was left within the testing machine attachment ring. The bottom grip was manually turned until the specimen suffered a fracture. When this occurs, the bottom grip falls inside the attachment ring and the angle was subsequently measured by a digital angle measurement device. The measurements were performed at room temperature. Three specimens of the each sample set were tested, and an average value was reported.

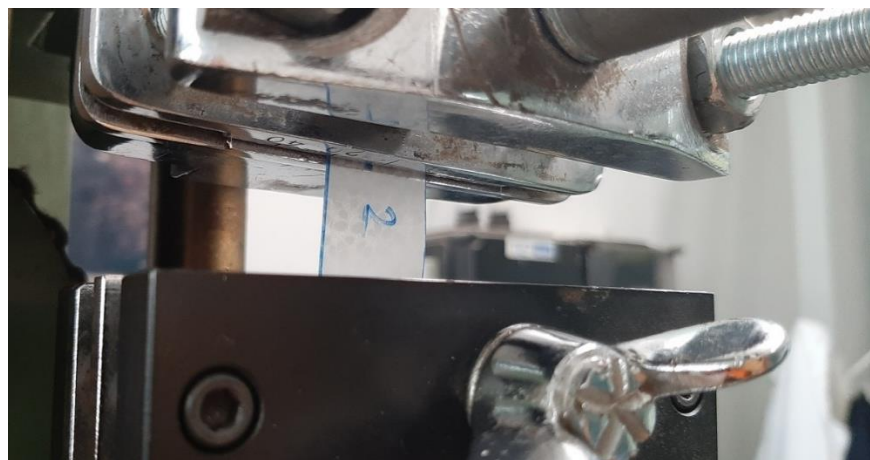


**Figure 3.** Measurement the angle of torsion.

### **Differential scanning calorimetry (DSC)**

The thermal properties of polymer blends were investigated using the differential scanning calorimeter (Q20 TA Instruments). Calibration was performed by Indium. The samples were analysed under a nitrogen atmosphere at a gas flow of 50 ml/min, in the temperature range from 5 to 250 °C, at a heating rate of 10 °C min<sup>-1</sup>. The glass transition temperature was determined as an inflection point.

### **Thermogravimetric analysis (TGA)**

Thermal degradation of polymer films was investigated using the LECO 701 Thermogravimetric Analyzer. Measurements were carried out under the air flow (50 ml/min) in the temperature range from 25 to 800 °C at a heating rate of 10 °C/min.

### **X-ray diffraction (XRD)**

The phase analysis of polymer blends was investigated by the Philips PW1820 X-Ray diffractometer, using CuK $\alpha$  radiation (experimental setup of 30 kV and 30 mA). The data covers the 10-40 ° angular range. The degree of crystallinity was estimated using the Hermans - Weidinger method,<sup>28</sup> and the MDI Jade software package. The distance between polymer chains in amorphous phase ( $\langle R \rangle$ ) for polymer blends was calculated using Equation 6,<sup>29</sup> considering the position of amorphous halo:

$$\langle R \rangle = \frac{5}{8} \left( \frac{\lambda}{\sin \theta} \right) \quad (6)$$

where  $\lambda$  (0.154 nm) is the wavelength of the radiation, and  $2\theta$  is an angle of diffraction.

### **Investigation of antimicrobial activity**

For test microorganisms were chosen referent strains of food-borne bacteria: *Escherichia coli*, *Salmonella* Typhimurium, *Listeria monocytogenes*, *Staphylococcus aureus*, as well as yeasts and fungi references: *Saccharomyces cerevisiae*, *Candida albicans*, and *Aspergillus brasiliensis*. All strains were obtained from American Type Culture Collection (ATCC) and stored at -72 °C. Prior to use, microorganisms were incubated at Plate Count Agar (PCA, HiMedia, Mumbai, India) or Sabouraud Dextrose Agar (SDA, HiMedia, Mumbai, India), respectively.

In order to assess of antimicrobial activity of pure essential oil, the disk-diffusion method reported in detail by Riabov et al.<sup>30</sup> was selected. Briefly, freshly prepared suspensions of each microorganism (approx. 6 log CFU/mL) were used, while the tested volume of LG was 10  $\mu$ L was applied into sterile cellulose-based disks in triplicate. After the incubation period, the inhibition effect was measured as diameters of the obtained zone around disks. The obtained results based on diameters of inhibition zone can be interpreted as the following: <22 mm = resistant; 22-26 mm intermediate; >26mm sensitive microorganism on tested sample. The sterile distilled water was a negative control, while antibiotic (chloramphenicol (30 mcg)) and antimycotic (3%

cycloheximide) were positive controls. Additionally, minimal inhibitory concentration (MIC) for all sensitive microorganisms was determined by microdilution methods<sup>31</sup> using original LG oil (as 100%), and a series of dilutions prepared in 5% DMSO (50, 25, 12.5 ... 0.195, 0.0975% v/v). In order to evaluate the pharmacodynamic potential of the antimicrobial effect of the determined MICs, the time-kill study was done. Aćimović et al.<sup>32</sup> have described in detail time-based monitoring of the antimicrobial effect of MICs during contact with sensitive microorganisms. Contact times were maximum of 24 hours for bacteria, and 72 hours for yeast and fungi, while sampling was done in ten points during the mentioned period. Comparatively, non-treated bacterial suspension was incubated under the same conditions.

In order to determine antimicrobial effect during direct contact of microbial cells and the prepared CA/PCL-diol 10% films (control and 3, 5, 7% LG addition), the previously mentioned disk-diffusion was selected, but with one main modification. Instead of sterile cellulose-based disks (for application of essential oil), prepared films are cut in the shape of a disk of the same diameter (6 mm) as the commercial disks and applied on the inoculated nutrient media. All analyses were done in triplicate.

### **Preliminary assessment of fresh fruit packaging efficiency**

In order to assess the efficiency of biological activities of the formed blends, the grapefruit (*Citrus paradisi* Macf.) slices are packed in the improvised packaging system in such a way that the entire surface of the grapefruit slice was in direct contact with the packaging material (Figure 4). The fresh untreated and washed grape fruits are selected for the test, and cut and drained in sterile conditions in order to obtain equal slices (diameter 90 mm, thickness 6 mm). Each slice was put in a suitable holder (height 5 mm). After artificial contamination by *A. brasiliensis* spores ( $10^4$  CFU/mL) using 5 points on slice surface, CA/PCL blends (control and LG) have served for packaging of each holder with slice. The blends were placed on the contaminated surface of the grapefruit and then the maximum tightening was performed (the difference in height between the slice and the holder allowed complete contact between the packaging and the fruit surface). The adhesive tape was added to insure the obtained system conditions. All samples were stored on  $15 \pm 1^\circ\text{C}$  for 10 days, while sampling was done after 1, 3, 5, 7 and 10<sup>th</sup> storage days. Prior imaging, slices were unwrapped for better monitoring of fungal growth on samples. Additionally, assessment of antimicrobial treatment was done by counting the squares with fungal growth using

formed network (Figure 4). The network allows a systematic approach when the overgrown surface has to be rated by the naked eye. After unwrapping, the formed network was placed onto the grapefruit slice and counted the squares with growth in them. The number of squares with fungal growth was correlated with the percent of the visible growth after each sampling time.

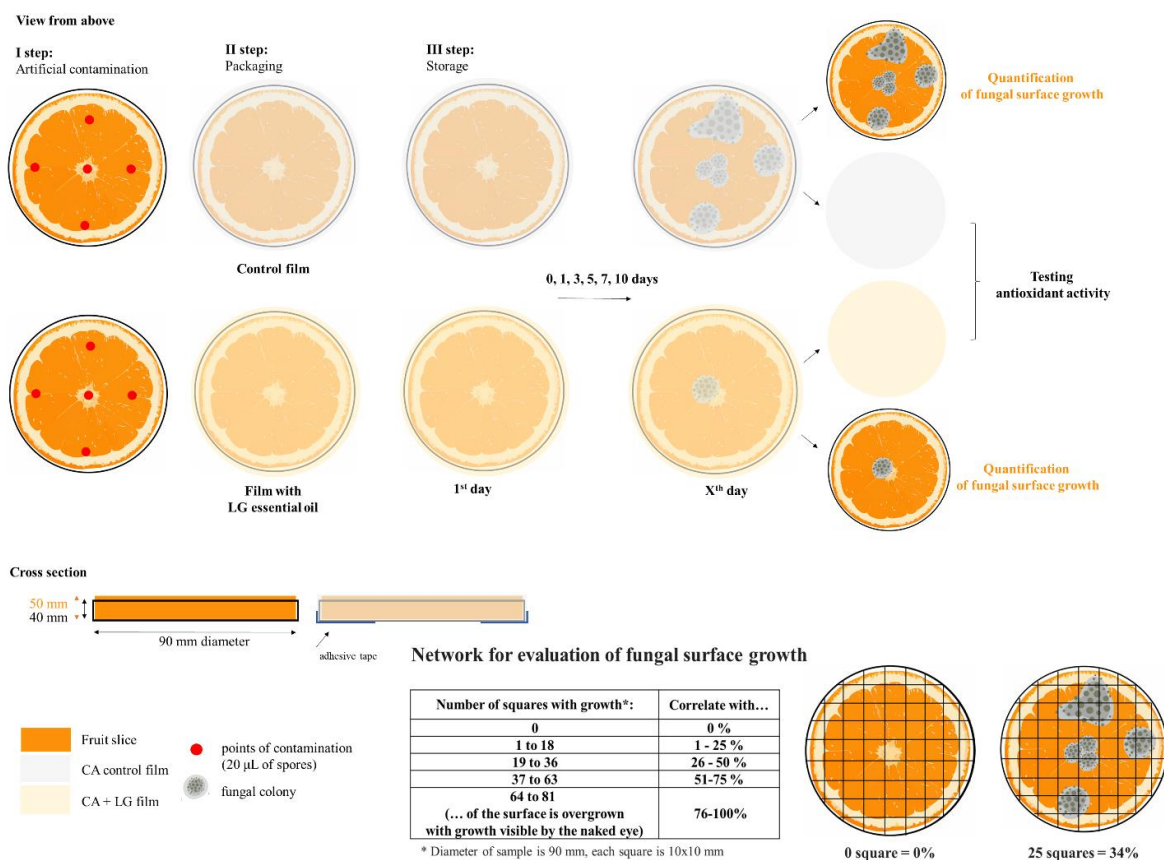


**Figure 4.** Experimental set-up for evaluation of packaging efficiency.

## Results and Discussion

### Results of FTIR analysis

FTIR spectra of polymer blends without (a and b) and with essential oil (c) as well as the spectrum of pure lemongrass oil (d) and compatibilizer (e) are presented in Figure 5. A broad peak from 3600 to 3350  $\text{cm}^{-1}$  presented in the spectra of blends is assigned to the OH stretching of the cellulose acetate and PCI-diol. In FTIR spectrum of compatibilizer, two peaks at 3410 and 3324  $\text{cm}^{-1}$  correspond to the stretching of secondary hydroxyl group of tartaric acid and OH group of

carboxylic acid. In FTIR spectrum of a neat lemongrass oil peak which shows the presence of OH group appears at  $3473\text{ cm}^{-1}$  (citronellol, nonan-4-ol). Peaks between  $2900$  and  $2500\text{ cm}^{-1}$  in the spectra of blends and compatibilizer correspond to the C-H stretching in PCL-diol and compatibilizer, respectively. In the FTIR spectra of the neat oil peaks which correspond to C-H stretching appear at  $2969$ ,  $2926$ ,  $2912$ , and  $2857\text{ cm}^{-1}$ .

The peak at  $1720\text{ cm}^{-1}$  is visible in all spectra and it is attributed to the ester bond in cellulose acetate, polycaprolactone diol chain, plasticizer, and lemongrass oil. This peak in the plasticizer spectrum confirms that reaction esterification has been successfully performed between tartaric acid and glycerol. A strong peak at  $1673\text{ cm}^{-1}$  is attributed to the unsaturated conjugated C=O group present in the citral. Small peaks at  $1634$ ,  $1617$ , and  $1442\text{ cm}^{-1}$  in the spectrum of essential oil are attributed to the C=C stretching. The band at  $1470\text{ cm}^{-1}$  in the spectrum of blends is assigned to -CH deformation, while the band at  $1420\text{ cm}^{-1}$  visible in spectra of blends and compatibilizer is attributed to C-O-H bending. A strong peak at  $1366\text{ cm}^{-1}$  in FTIR spectra of polymer blends corresponds to C-O-H stretching in pyranose. Peaks at  $1294$ ,  $1233$ ,  $1187$ , and  $1034\text{ cm}^{-1}$  correspond to O-C stretching in ester groups. In the spectrum of compatibilizer, there is a peak at  $1202\text{ cm}^{-1}$  which is assigned to O-C stretching from the carboxylic group; two peaks at  $1184$  and  $1085\text{ cm}^{-1}$  correspond to O-C and C-C-O stretching of ester groups. In the FTIR spectrum of lemongrass oil, in this range there are peaks which correspond to the O-H stretching ( $1377$ ,  $1194\text{ cm}^{-1}$ ), C=C vibrations ( $1155$  and  $1120\text{ cm}^{-1}$ ) and stretching of ester group ( $1043\text{ cm}^{-1}$ ). A weak peak in the range from  $985$  to  $961\text{ cm}^{-1}$  visible in all spectra corresponds to the C-O stretching of hydroxyl group. An expressed peak in plasticizer spectrum at  $890\text{ cm}^{-1}$  and the weak peaks in the range between  $790$  and  $732\text{ cm}^{-1}$  of all samples correspond to C-H bending. The addition of plasticizer does not affect the changes in the FTIR spectrum (Figure 5a, b and c). However, the inclusion of lemongrass oil in the blend composition results in additional peaks between  $2970$  and  $2800\text{ cm}^{-1}$  in the FTIR spectrum - five peaks at  $2944$ ,  $2921$ ,  $2895$ ,  $2864$  and  $2850\text{ cm}^{-1}$  instead of three at  $2944$ ,  $2922$  and  $2864\text{ cm}^{-1}$  in the FTIR spectrum of blends without added essential oil (Figure 5 a and b).

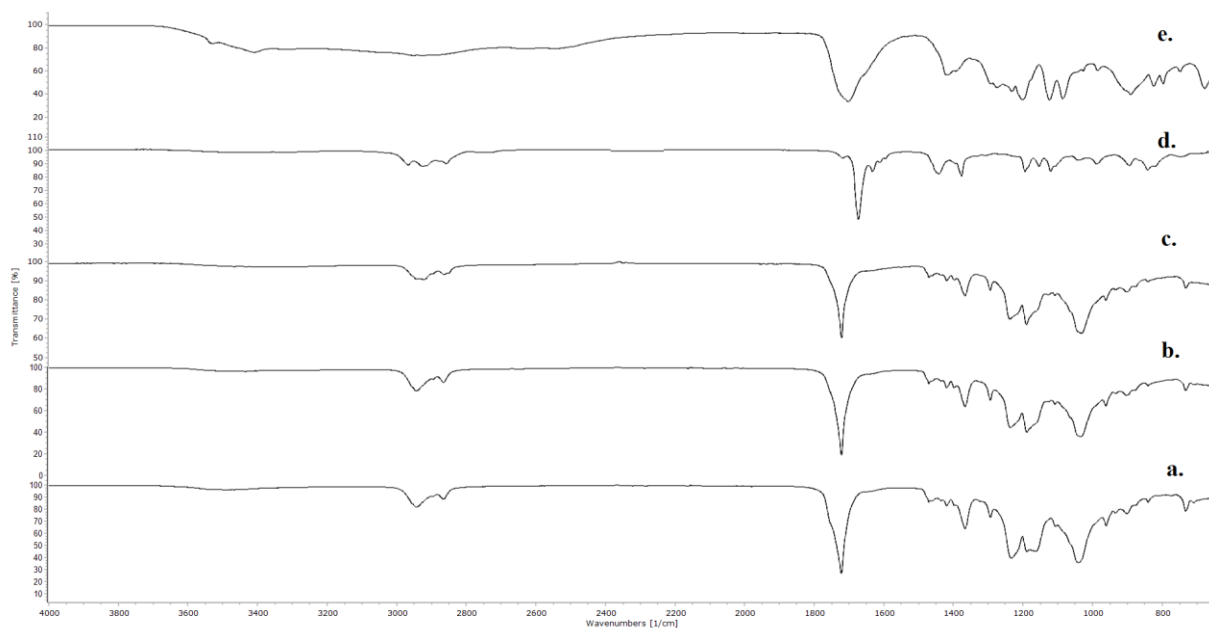


**Figure 5.** FTIR spectra of a) CA/PCL 0% blend, b) CA/PCL 10% blend, c) CA/PCL 10%, 5% LG blend, d) lemongrass oil, e) GTT plasticizer.

### Results of scanning electron microscopy (SEM) analysis

Figure 6 shows the scanning electron micrographs of the top surface (a) and cross-section (b) of CA/PCL-diol blends with different amounts of plasticizer (Figure 6I, II, III), as well as of pure CA (Figure 6IV), and CA with plasticizer (Figure 6V). Pure CA, with and without plasticizer possesses a smooth surface. The used plasticizer acts as a compatibilizer, which is evident according to the nature and number of pores. Therefore, blend without GTA (Figure 6Ia and b) possesses the greatest number of pores, which are deep and non-uniformly distributed; the cross-section demonstrates segregation of CA and PCL-diol; the formation of pores could be the consequence of the existence of voids between polymer chains of CA and PCL-diol, as a result of significantly stronger cohesion forces than adhesion ones. Both polymers are highly soluble in acetone, therefore, their chains take conformation of a random coil that occupies space with a larger radius. Random coils of CA and PCI-diol permeate each other, and space between them after acetone evaporation creates a pore. The addition of plasticizer/compatibilizer leads to a better mixing of polymers which results in decreasing in pores number and depth, acting as a biding agent between CA and PCL-diol, which is particularly visible in the cross-section (b), which with the addition of plasticizer takes over more regular honeycomb-like structure.



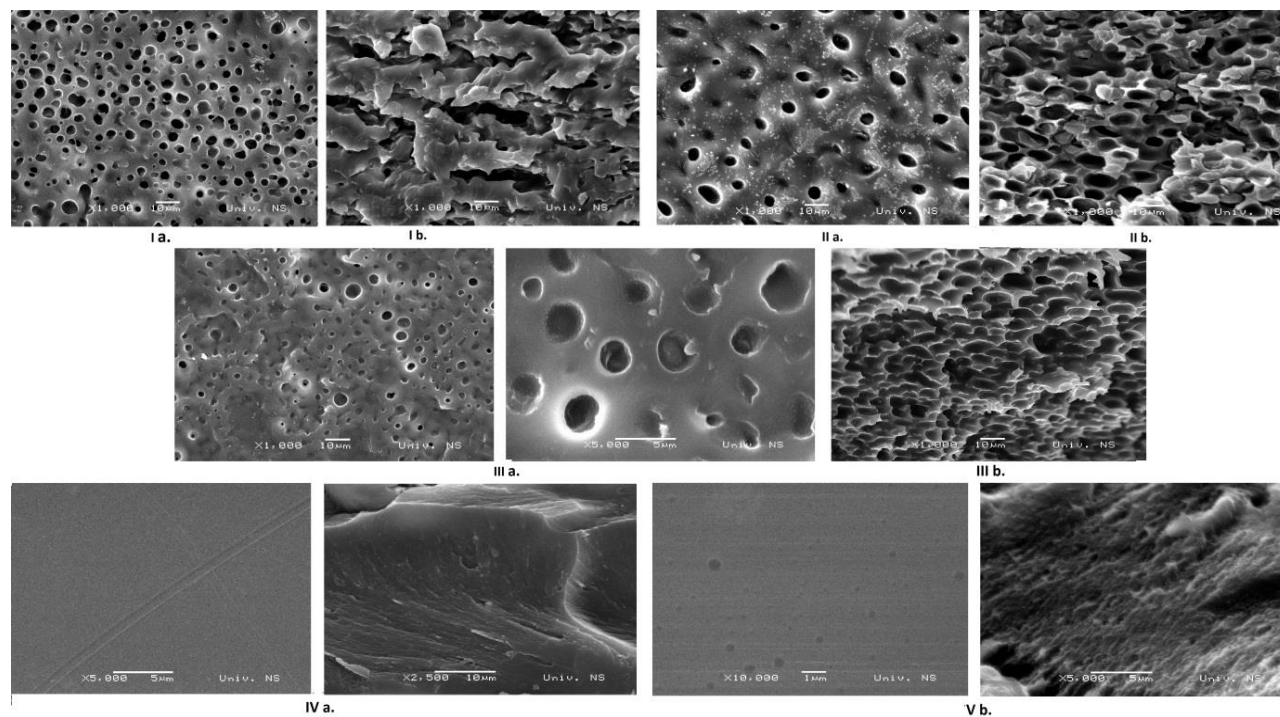


**Figure 6.** SEM micrographs of top surface (a) and cross-section (b): I CA/PCL-diols 0%, II CA/PCL-diols 5%, III CA/PCL-diols 12%, IV neat CA, V CA 10%

### Surface energy measurements

The results of the surface energy of polymer blends give the information about miscibility of their compounds.<sup>33</sup> The results of contact angle measurements and calculated surface energy for the virgin polymers and polymer blends with different amounts of plasticizers are presented in Table 2. Increasing plasticizer amount leads to the increase of surface energy of polymer blends, as a result of better compatibilization and hydrophilic nature of plasticizer. Virgin polymers have similar values of surface energy, which are above the surface energy values of the polymer blends. Adding plasticizer/compatibilizer results in better wetting between polymer blends and used solvents (lowering in contact angle), which is the consequence of compatibilizer hydrophilic nature. Therefore, the greatest value of surface energy has been recorded for the polymer blend with 12 wt% of compatibilizer (31.04 mN/m), whose greater amount comes from the polar interactions. The addition of lemongrass oil in blend composition does not affect significantly surface energy. However the addition of oil in an amount of 7 wt% results in the increase of surface energy which comes from non-polar interactions, which is expected considering the hydrophobic nature of the essential oil.

**Table 2.** Contact angle and surface energy values for CA/PCL - diol polymer blends with a different amount of plasticizer/compatibilizer.

Sample	Contact angle (°)		Surface energy (mN/m)		
	$\theta_1$	$\theta_2$	$\gamma_s$	$\gamma_s^p$	$\gamma_s^d$
CA/PCL 0%	69.4	65.1	33.67	21.62	12.05
CA/PCL 5%	67.2	64.8	35.04	24.20	10.84
CA/PCL 7%	65.3	62.1	41.41	26.53	14.89
CA/PCL 10%	59.7	56.9	42.00	28.31	12.89
CA/PCL 12%	55.8	53.2	44.41	31.04	13.37
CA/PCL 10%, 3% LG	60.2	56.3	41.12	28.94	12.18
CA/PCL 10%, 5% LG	62.4	56.1	39.80	23.72	16.08
CA/PCL 10%, 7% LG	66.2	53.3	40.06	15.36	24.70
CA 10% <sup>a</sup>	50.6	48.4	48.62	34.83	13.79
CA neat	56.2	53.3	44.05	30.25	13.80
PCL diol	57.03	54.6	45.83	31.92	11.91

<sup>a</sup> CA with 10 wt% of plasticizer

### Moisture content, total soluble matter and water vapour transmission rate analysis

Moisture content decreases with addition of 5 wt% of plasticizer, because of decreasing the number of pores (results of SEM analysis) and better adhesion between two polymers in the presence of plasticizer/compatibilizer (Table 3). Further addition of plasticizer leads to increasing in MC value, due to its hydrophilic nature. In series prepared by variation of essential oil, addition of lemongrass oil does not affect a MC value in lower concentrations, but addition in concentration of 7 wt% leads to the decreasing of MC from 9.41 (for the control sample CA/PCL/diol 10%) to the 8.21% (for CA/PCL 10%, 7% LG), due to the hydrophobic nature of essential oil.

TSM values of films are especially important in packaging of food with a great amount of water such is fruit. Obtained blends with lower amounts of plasticizer (0-7 wt%) do not possess solubility in water (Table 3). Addition of plasticizer in amount of 10 and 12 wt% results in low solubility of polymer blends, as a consequence of hydrophilic and water -soluble plasticizer. Lemongrass oil added in investigated amounts does not significantly affect a TSM value in comparison to control film.

WVTR is important parameter for food packaging, because of the significant role of water in microbial stability and reactions which lead to the deterioration of product quality.<sup>34</sup> Blend without plasticizer possess the greatest WVP value, due to the phase segregation and porosity structure.

Addition of plasticizer in amount up to 7 wt% leads to the decreasing in WVP (Table 3). Further addition in plasticizer amount result in slightly increasing in WPV. Addition of lemongrass oil in amount of 7 wt% results in increased WVP in comparison to the control sample. The gas permeability of polymer is influenced by crystalline – amorphous phase ratio, wherein the crystalline phase is impermeable to gases, and the greater amount of amorphous phase results in better gas permeability.<sup>35</sup> Lemongrass oil in amount of 7 wt% acts as a plasticizer, increasing the mobility of polymer chains and polymer-oil interaction which results in increasing of WVP value.<sup>36</sup>

**Table 3.** Moisture content (MC), (total soluble matter) TSM and water vapour transmission rate (WVTR) values for polymer blends with different amounts of plasticizer and lemongrass oil.

Sample	MC (%)	TSM (%)	WVTR (g/m <sup>2</sup> h)
CA/PCL - diol 0%	6.16	-6.89	106.22
CA/PCL – diol 5%	3.88	-2.79	87.08
CA/PCL - diol 7%	5.59	-2.76	66.96
CA/PCL – diol 10%	9.41	1.24	70.53
CA/PCL - diol12%	10.33	2.98	73.45
CA/PCL - diol 10%, 3% LG	9.35	1.12	70.23
CA/PCL – diol 10%, 5% LG	9.27	1.09	71.26
CA/PCL - diol 10%, 7% LG	8.21	1.00	75.67

### Mechanical analysis and film thickness

The thickness values for films used for packaging formation are given in the first column of Table 4, and in the fourth column for the films subjected to the determination of torsion resistance. Tensile strength and elongation at break values are similar and rise with increasing in compatibilizer/plasticizer amount. The addition of lemongrass oil in amounts of 3 and 5 wt% per weight of blend does not have an effect on the tensile strength, but the addition of the lemongrass oil in the amount of 7 wt% results in improved tensile strength in comparison with the control blend. The used oil is compatible with blend and in this amount has a function of plasticizer, which can be concluded according to the improved value of elongation at break. The angle of torsion increases with increasing plasticizer amount which is in coherence with tensile properties. Therefore, the sample CA/PCL-diol 12% has demonstrated the greatest value of angle (107.40 °),

while the lowest one was recorded for the blend without plasticizer (65.90 °). Variation of the essential oil amount in series with the same composition, it can be observed that the angle of torsion increases with increasing in LG oil amount, but this increase is not significant for lower amounts of etheric oil.

**Table 4.** Results of thickness, tensile strength (TS), elongation at break (EB) and the angle of torsion.

Sample	Thickness (µm)	TS (MPa)	EB (%)	Thickness (µm)	The angle of torsion (°)
CA/PCL – diol 0%	169.3 ± 0.013	20.31 ± 2.56	4.82 ± 1.28	170.0 ± 0.012	65.9 ± 2.40
CA/PCL – diol 5%	182.7 ± 0.074	20.36 ± 3.60	6.56 ± 2.27		72.30 ± 3.11
CA-PCL – diol 7%	156.0 ± 0.021	23.00 ± 4.25	9.18 ± 2.34		79.50 ± 2.13
CA/PCL – diol 10%	174.5 ± 0.008	23.56 ± 1.91	10.17 ± 4.02		84.70 ± 1.45
CA/PCL – diol 12%	184.1 ± 0.007	24.84 ± 2.68	11.72 ± 2.52		107.40 ± 3.16
CA/PCL – diol 10%, 3% LG	174.5 ± 0.007	21.29 ± 1.17	10.23 ± 3.35		85.26 ± 2.67
CA/PCL – diol 10%, 5% LG	175.0 ± 0.011	21.79 ± 3.32	10.79 ± 3.12		87.10 ± 1.85
CA/PCL – diol 10%, 7% LG	174.5 ± 0.014	24.91 ± 4.49	11.28 ± 2.92		98.03 ± 2.85

### DSC analysis

DSC thermograms of polymer blends are presented in Figure 7. Increasing the amount of plasticizer in polymer blends leads to the decrease of glass transition temperature – from 34 °C for polymer blend without plasticizer, to 31 °C for polymer blend with the greatest amount of plasticizer (CA-PCL-diol 12%). The glass transition temperature of blends is between the glass transition temperatures of virgin polymers, which are -56 °C for PCL diol (Figure S1, Supporting information) and 206 °C for CA (Figure S2, Supporting material). The first melting peak appears

at 43-46 °C, and corresponds to the melting of PCL-diol in the blend. The other melting peak, at 208-209 °C is assigned to the melting of CA in the polymer blend. The addition of GTT does not affect significantly a glass transition temperature, leading to its decreasing only for 5 °C at the greatest investigated amount (12 wt%). This has confirmed that GTT does not have strong plasticizing effect, but acts more as a compatibilizer between polymers in blend, which is confirmed by results of SEM and WVTR measurements. The presence of lemongrass oil in polymer blend in an amount of 7 wt% does not affect significantly the phase transitions of polymer blend (Figure 7f). Peaks which appear at 167 and 183 °C are attributed to the essential oil evaporation.

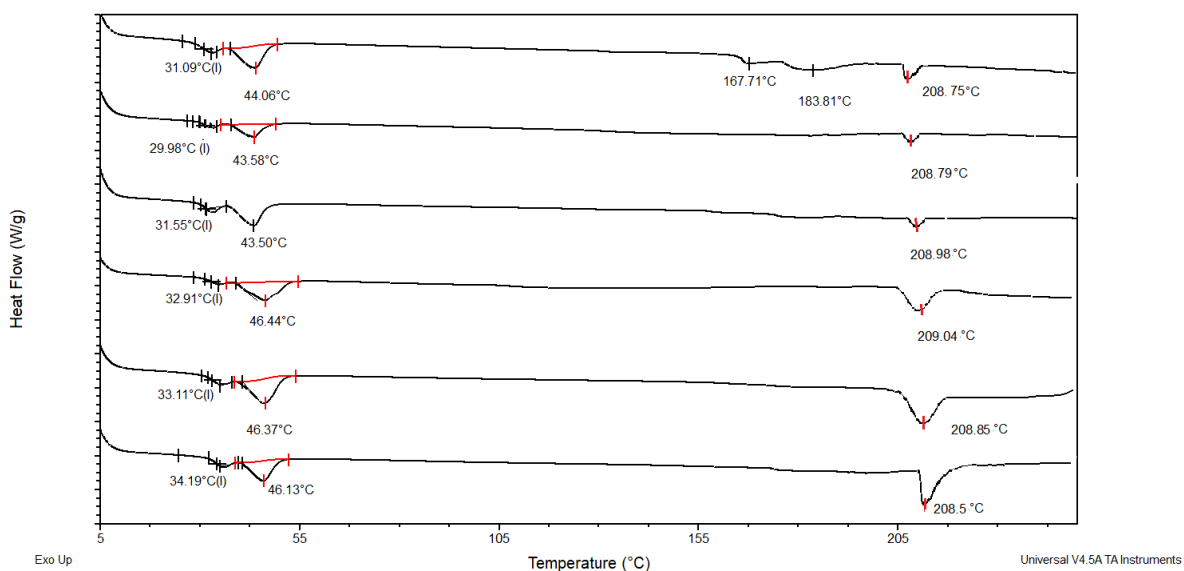


**Figure 7.** DSC curves of polymer blends: a) CA/PCL-diol 0%, b) CA/PCL - diol 5%, c) CA/PCL - diol 7%, d) CA/PCL - diol 10%, e) CA/PCL -diol 12%, f) CA/PCL diol 12%, 7% LG.

### Thermal gravimetric analysis (TGA)

TGA curves of the virgin polymers (CA and PCL-diol) and polymer blends with and without essential oil are presented in Figure 8, and the results obtained from the derivative thermogravimetric curve (DTG) are summarised in Table 5. The DTG curves are given in Supporting information (Figure S3, S4, S5, S6). Degradation of a neat CA and blends is carried out in three steps, where the second step is evidenced as a main thermal decomposition event. The first step, up to 317 °C, in the thermogram of neat CA corresponds to the mass loss of 6% due to

the elimination of moisture and deacetylation.<sup>37, 38</sup> The second step, up to 425 °C with a mass loss of 82% is attributed to the degradation of the CA main chain, the breakdown of the glycosidic linkages, and the formation of furanic compounds.<sup>39</sup> The third stage, up to 767 °C corresponds to the complete degradation and sample carbonation until 0.1% of the residual mass. The TGA curve of PCL-diol displays one degradation step,<sup>40</sup> with a maximal degradation rate at 427 °C. The first degradation stage in the thermogram of the blend, which ends up at 277 °C is assigned to the mass loss of 8% due to the elimination of moisture, deacetylation. In the second, main degradation stage, up to 449 °C, blend loss 87% of weight, due to the degradation of CA main chain and breaking of the ester linkages in the PCL-diol chain. The third stage is a result of the final degradation and sample carbonation ending up with a residual mass of 0.12%. A combination of CA and PCL-diol in this ratio in polymer blend results in a material with a little bit of thermal stability in comparison to the virgin polymers, which is manifested in the longer second and third phases. Incorporation of lemongrass oil in the polymer blend results in a four-step degradation process, where the first step up to 172 °C corresponds to degradation of lemongrass oil, moisture loss, resulting in weight loss up to 6%.<sup>41</sup> The second step, up to 277 °C is attributed to deacetylation. Further decomposition is carried out in a similar way as decomposition of polymer blend without oil.

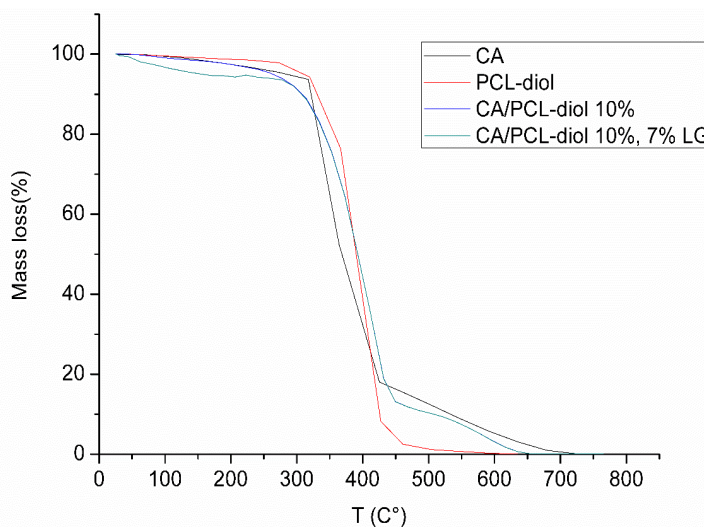


**Figure 8.** TGA thermograms of neat CA, PCL-diol, CA/PCL-diol 10% and CA/PCL-diol, 7% LG

**Table 5.** DTG peak maxima values for neat CA, CA/PCL-diol 10% and CA/PCL-diol, 7% LG

Sample	T <sub>5%</sub> (°C)	T <sub>dmaxI</sub> (°C)	T <sub>dmaxII</sub> (°C)	T <sub>dmaxIII</sub> (°C)	T <sub>dmaxIV</sub> (°C)	Residual mass
CA	270.3	131.6	364.0	545.9	/	0.1
CA/PCL – diol 10%	258.3	105.7	431.6	597.1	/	0.12
CA/PCL – diol 10%, 7% LG	153.1	105.7	222.2	410.8	597.1	0.12

### XRD analysis

The wide-angle X-ray diffraction (WAXS) was used to investigate the level of polymer blends microstructure arrangement. Figure 9 illustrates the XRD patterns for polymer blends with different amounts of plasticizer. The results of crystallinity degree for polymer blends and neat polymers are presented in Table 6. In the XRD pattern of the neat PCL-diol (Figure 10), there are three intense reflections at  $2\theta = 21.30^\circ$ ,  $22.00^\circ$ , and  $23.60^\circ$ , and among investigated samples the highest degree of crystallinity is observed for the PCL-diol (28.80%). A broader reflection that appears in the diffractograms of polymer blends in the range from  $2\theta = 18.80^\circ$  to  $2\theta = 21.60^\circ$  is the consequence of amorphous contribution of blending with cellulose acetate.<sup>29</sup> Cellulose acetate is semi-crystalline polymer, in whose spectrum broad crystal peak is heavily overlapped with primary amorphous halo. Polymer blends have similar degree of crystallinity, in the range between 21.05 to 23.20%, which is in coherence with the results of DSC analysis. The average interchain spacing,  $\langle R \rangle$ , rises with the addition of plasticizer in the amount of 5 wt%. Further increase in plasticizer amount leads to the decrease in  $\langle R \rangle$  value, which implies more efficient chain packing and compatibilizing effect of plasticizer.

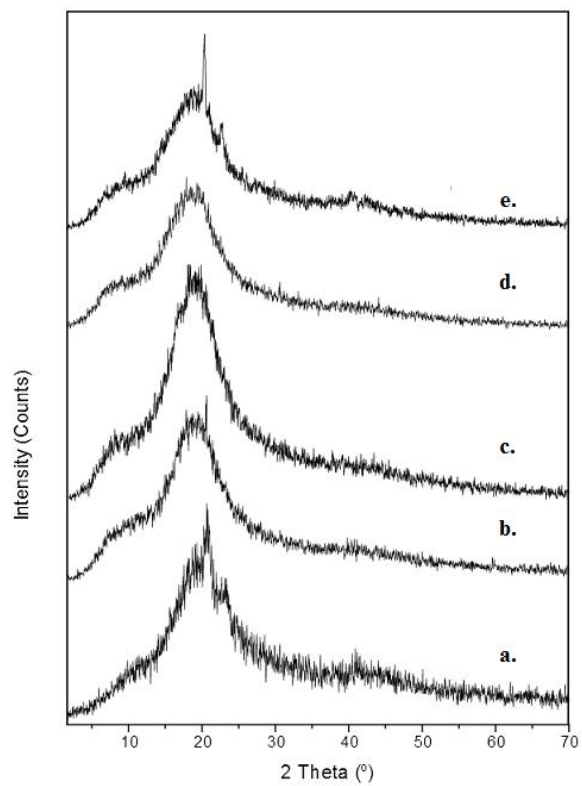


**Figure 9.** XRD patterns of polymer blends with different amount of plasticizer: a) CA/PCL - diol 0%, b) CA/PCL – diol 5%, c) CA/PCL – diol 7%, d) CA/PCL - diol 10%, CA/PCL - diol 12%

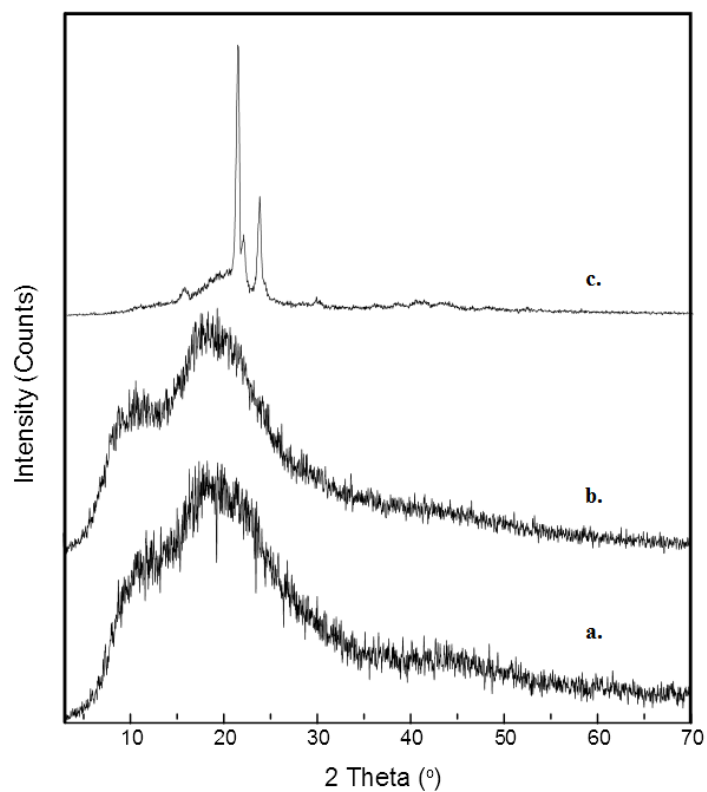




**Figure 10.** XRD patterns of: a) neat CA, b) CA 10%, c) neat PCL-diol**Table 6.** Degree of crystallinity and interchain spacing (<math>\langle R \rangle</math>) for polymer samples

Sample	Cristallinity (%)	<math>\langle R \rangle</math> (Å)
CA-PCL – diol 0%	21.05	5.54
CA-PCL -diol 5%	20.86	5.68
CA-PCL - diol 7%	23.20	5.60
CA-PCL -diol 10%	22.78	5.33
CA-PCL -diol 12%	22.16	5.21
CA 10%	19.70	5.46
CA neat	21.81	6.15
PCL diol	28.80	/

### Antimicrobial properties

According to the obtained results of the disk-diffusion test (Figure 11a), LG essential oil has shown a low antimicrobial activity against both tested Gram-negative bacteria *Escherichia coli* ATCC 25922 and *Salmonella* Typhimurium ATCC 1331. On the other hand, a very high antimicrobial activity was observed against Gram-positive bacteria *Staphylococcus aureus* ATCC 25923 and *Listeria monocytogenes* ATCC 35152. The gained inhibition zone for these two bacteria is higher than for chloramphenicol, which indicates the strong antimicrobial potential of LG essential oil for preventing of propagation of bacterial growth in the presence of an adequate amount of oil. Furthermore, inhibition of growth in the presence of LG oil was also observed for all tested yeasts and fungi (*S. cerevisiae* ATCC 9763, *C. albicans* ATCC 10231, and *A. brasiliensis* ATCC 16404). Compared with cycloheximide as an antimycotic agent, the obtained zones are at the same or higher level in the case of LG essential oil. It can be concluded that using LG essential oil against yeast and fungal contamination is promising, but the further investigation can be directed on testing a larger number of food contamination isolates, not only referent strains. For the determination of the minimal concentration of LG essential oil that inhibits the growth of the sensitive microorganisms, minimal inhibitory concentration (MIC) was determined (Figure 11b). The MIC

value of 0.39 % (v/v) for *S. aureus* represents the lowest obtained value, while the total inhibition of *L. monocytogenes* was achieved using 0.78% (v/v) of tested oil. For both tested yeasts, MICs value is 1.56% (v/v), which suggests that eukaryotic cells are more resistant to the tested antimicrobial agent. This observation is in accordance with the obtained MIC value 3.125% (v/v) for *A. brasiliensis*, which is 8- and 4-times higher than for *S. aureus* and *L. monocytogenes*, respectively. When it comes to application antimicrobial agent into packaging material, a very important view of antimicrobial activity is the time-based monitoring of inhibition effect, i.e., pharmacodynamics potential of MIC value of LG essential oil during contact time between antimicrobial agent and microbial cells. Therefore, the pharmacodynamic potential was determined by the time-kill kinetics study method, following antimicrobial effect during 24 hours for sensitive bacteria (Figure 11c), and 72h for yeasts and fungi (Figure 11d). Parallel to the set experiment, non-treated bacterial suspensions were incubated at the same incubation conditions to perceive microbial behaviour without the addition of MIC values of the LG essential oil. Both graphs (Figure 11c and 11d) represent growth profiles curves which indicated the number of viable cells over the defined contact or incubation time. For non-treated suspensions, the obtained curves have an expected S-shape, with noticeable growth stages during microbial reproduction: lag, log, and stationary, with the increase of cell number in the range of 1.5 and 3 log CFU/mL. On the contrary, the obtained curves for MIC value indicate biocide effect for *S. aureus* and *L. monocytogenes* after a contact time of 8 and 12 hours, respectively, while the same effect was observed for both yeasts for 18 hours. A fungicide effect was achieved in six hours shorter time for *A. brasiliensis*. Interestingly, the effect of MIC concentration lasted until the end of the contact time, indicating that the applied concentrations certainly have a biocidal effect on all cells. In other words, the applied concentration of LG essential oil is present during the whole contact time which prevents injured cells to resume. In summary, it can be concluded that the contact time of 18 hours between LG essential oil in a concentration above 3.125% (v/v) and sensitive microorganisms are certainly enough for complete inhibition of all tested microorganisms present in a concentration of approx. 5 log CFU (initial concentration in the experiment).

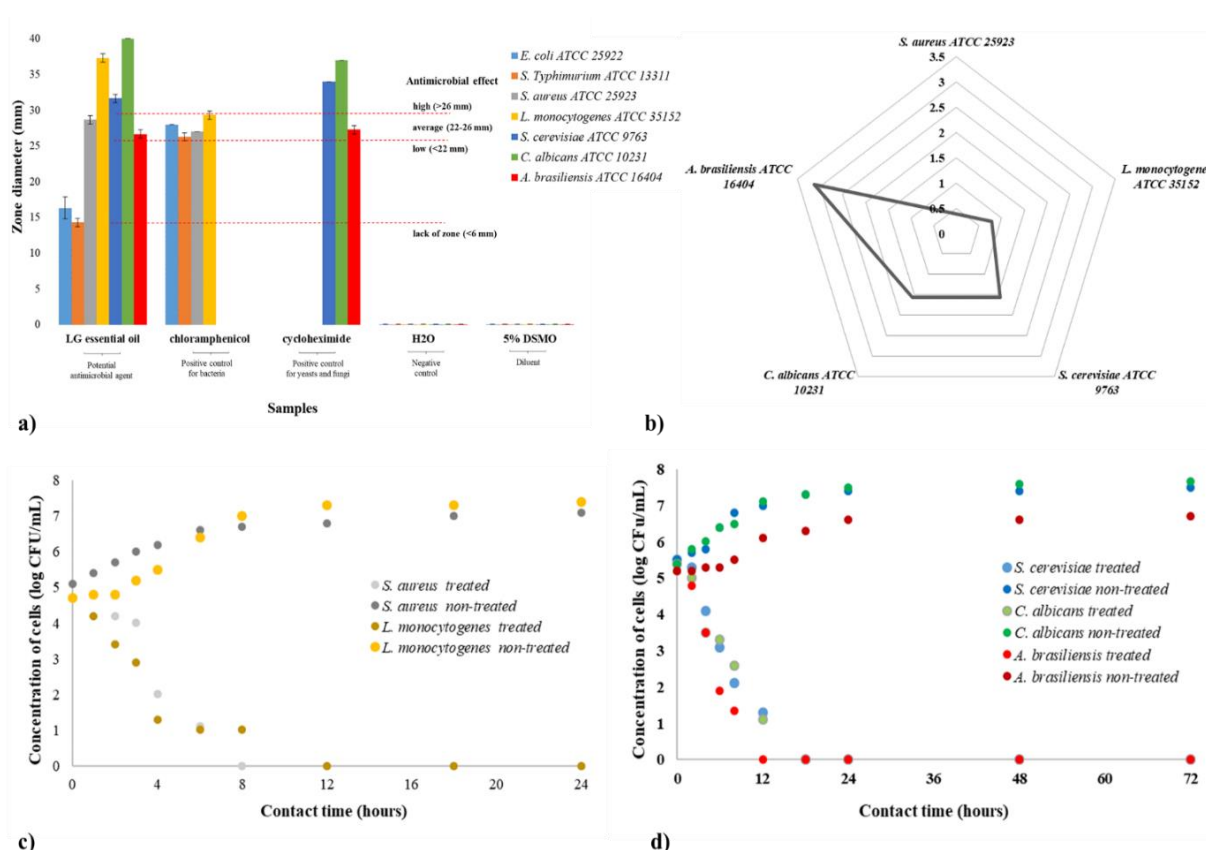


**Figure 11.** a) Inhibition zone; b) minimal inhibitory concentration (% v/v); c) time-kill kinetics study for sensitive bacteria; d) time-kill kinetics study for sensitive yeasts and fungi.

For a deep investigation of the antimicrobial effect of the prepared CA/PCL films, antimicrobial effects during direct contact between films and cells are evaluated (Figure 12). As control films, without LG essential oil did not express the inhibition of the tested microorganisms, the obtained values of antimicrobial activity can be attributed to the LG addition and successive release during contact time. Briefly, CA/PCL 10%, 3% LG has shown high antimicrobial effect against yeasts, but average or low effect against bacteria and fungi. The gained differences can be based on an insufficient amount of LG essential oil in the film, i.e., which did not release the MIC value for biocide effect against prokaryotic cells and fungi. A similar pathway was observed for CA/PCL 10%, 5% LG film, but with higher average values of the inhibition zone. CA/PCL 10%, 7% LG

films demonstrated a high antimicrobial effect of the tested material against all tested microorganisms. For a better understanding of different levels of antimicrobial effect, on Figure 10 are additionally a present difference in the inhibition zones obtained in the case of *A. brasiliensis*, where the addition of 3%, 5%, and 7 wt% LG showed a low, average, and high level of antimicrobial effect during contact time, respectively. It can be concluded that using 7% LG addition in films can inhibit all three types of microorganisms and releasing rate of antimicrobial agents is at a satisfactory level.

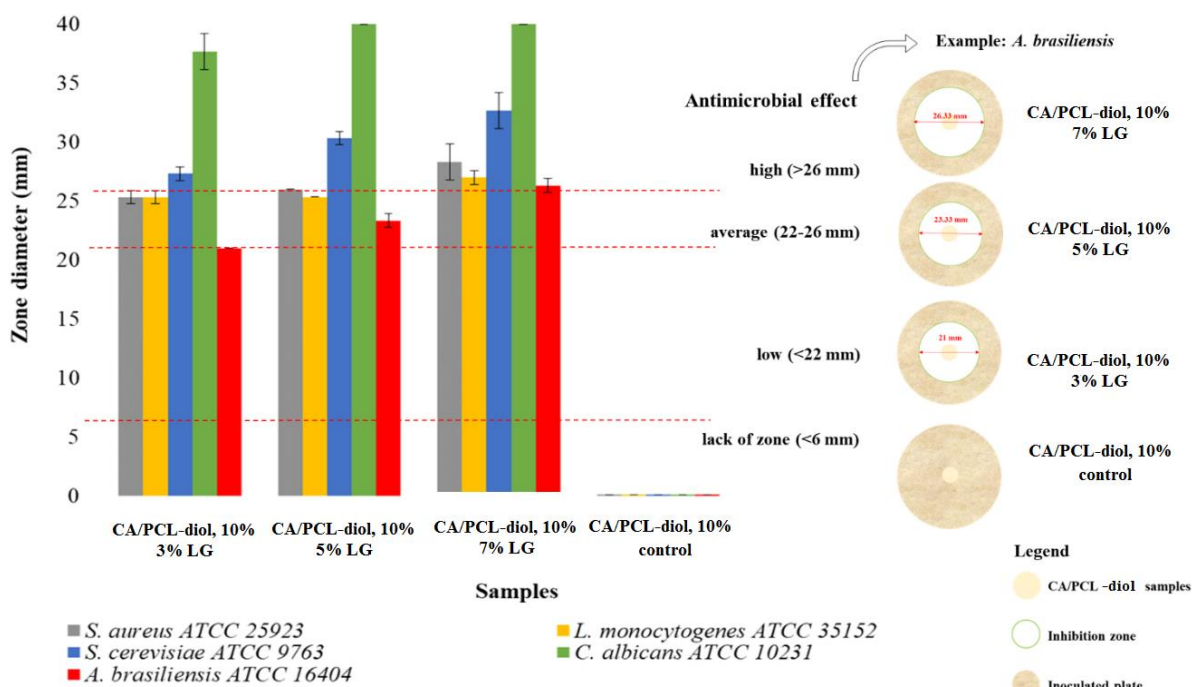


**Figure 12.** Antimicrobial effect of CA/PCL-diol samples.

### Preliminary assessment of the efficiency of fresh fruit packaging

As with all other citrus, grapefruits have to be harvested in full maturity, and cannot be stored at very low temperatures since the development of skin defects is almost inevitable.<sup>42</sup> Additionally, one of the usually microbial contaminations of grapefruits is directed to *Aspergillus* strains which cause a variation in skin colour and typical black mycelia on pulp and seeds.<sup>43</sup> Therefore, artificial

contamination by *A. brasiliensis*, which was previously defined as sensitive to lemongrass essential oil (Figure 11-12), was done using freshly sliced grapefruits. According to the obtained results of biological parameters (Table 7, Figure 13), the storage period can be prolonged for approximately double time. The sample with 7 wt% of LG was selected for preliminary assessment, considering the results of the disk-diffusion test and demonstrated optimal antifungal activity. The addition of 7% lemongrass essential oil into CA/PCL film is enabled to resist fungal growth better than control film alone, which suggests that the used antimicrobial agent in a concentration-dependent manner was as effective as remarkably reduced targeted fungi. The initial phase of fungal growth on control samples has seen with the naked eye on the third day of storage (5% of surface affected with visible contamination), while the same level of growth on fruit samples packaged on CA/PCL film with 7% LG was observed on the 7<sup>th</sup> day. This preliminary examination stopped after 10 days, due to the continued untenability of the fruit itself.

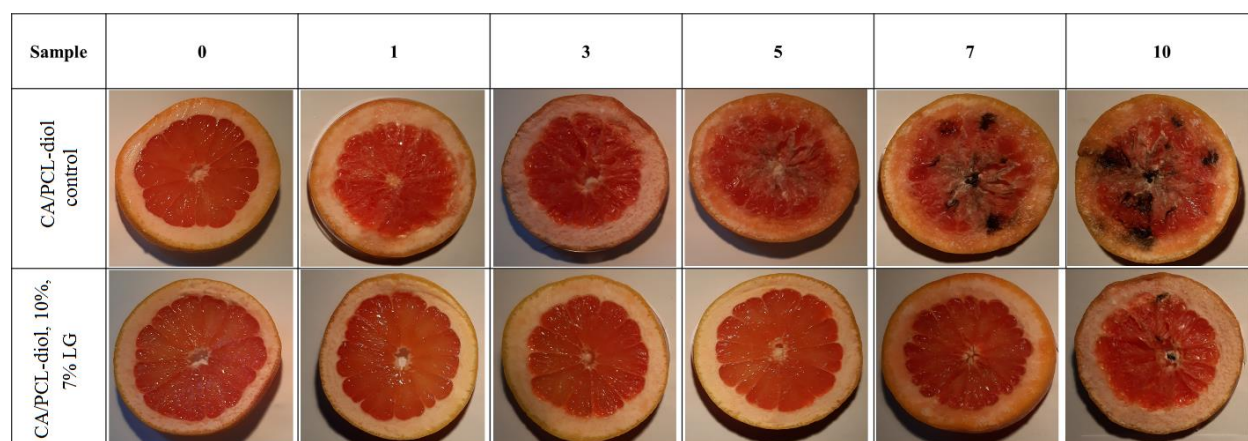


**Figure 13.** Photographs of grapefruit slice packed in CA/PCL-diol control or LG film during the storage period

Lemongrass essential oil was as effective as remarkably reduced fungi for 10 days of storage of grapefruits. Using LG as an antimicrobial agent incorporated in CA/PCL diol blends, control of microbial growth was achieved. The quality of grapefruits during storage has been limited by its perishable nature including specific conditions for storage and susceptibility to postharvest diseases associated with fungal contamination. In the current study, CA/PCL diol blends with 7% LG essential oil effectively inhibited or controlled targeted fungal populations.

**Table 7.** Assessment of the efficiency of fresh fruit packaging

Samples	CA/PCL - diol 10% control						CA/PCL –diol 10% 7% LG					
	0	1	3	5	7	10	0	1	3	5	7	10
Evaluation of surface affected with fungal growth (%)	0	0	5	40	70	85	0	0	0	0	5	10

## Conclusions

In a present work, a novel bio-based plasticizer glycerol tritartarate has been employed for the preparation of CA/PCL-diol films intended for fruit packaging. Used plasticizer has been showed compatibilizing effect, improving the miscibility of CA and PCL-diol. By addition of lemongrass essential oil in a film with optimized formulation (10 wt% of plasticizer) has been made a framework for obtaining of biodegradable active packaging, considering the results of disc-diffusion method and proved antimicrobial activity of lemongrass oil. Therefore, this sample has been used for preliminary assessment conducted with artificial contamination of grapefruit by *Aspergillus brasiliensis*, because *Aspergillus* strains cause a variation in skin colour and typical black mycelia on grapefruit pulp and seeds. Wrapping of grapefruit by film which contains 7 wt% of lemongrass oil results in significantly greater shelf life (extended 2.33 times), considering the fact that film without LG oil enables preservation for 3 days, when the first changes has been occurred, while the same level of fungal growth on the fruit samples packaged in CA/PCL film with 7% LG was observed on the 7th day. Obtained results have been provided the platform for manufacturing of biodegradable, cost – effective active packaging.

## Author Contributions

The manuscript was written through the contributions of all authors. All authors have approved the final version of the manuscript.

## Notes

The authors declare no competing financial interest.

## ACKNOWLEDGMENTS

The authors thank the Ministry of Education, Science and Technological Development, Republic of Serbia, project number 451-03-68/2022-14/ 200134, 451-03-9/2022-14/ 200134 and 451-03-68/2022-14/ 200222 for financial support.

## REFERENCES

1. De Kock, L.; Sadan, Z.; Arp, R.; Upadhyaya, P. A circular economy response to plastic pollution: Current policy landscape and consumer perception. *S. Afr. J. Sci.* **2020**, *116*, 1–2, DOI: 10.17159/sajs.2020/8097
2. Asgher M.; Qamar, S.A.; Bilal, M.; Iqbal, H.M.N. Bio-based active food packaging materials: Sustainable alternative to conventional petrochemical-based packaging materials. *Food Res Int.* **2020**, *137*, 109625 DOI: 10.1016/j.foodres.2020.109625
3. Jamieson, A.; J., Brooks, L. S. R.; Reid, W. D. K.; Piertney, S. B.; Narayanaswamy, B. E., and Linley, T. D. Microplastics and synthetic particles ingested by deep-sea amphipods in six of the deepest marine ecosystems on Earth. *Roy. Soc. Open Sci.* **2019**, *6*, :180667. DOI: 10.1098/rsos.180667
4. Ncube, L. K.; Ude, A. U.; Ogunmuyiwa, E. N.; Zulkifli, R.; Beas, I. N. Environmental Impact of Food Packaging Materials: A Review of Contemporary Development from Conventional Plastics to Polylactic Acid Based Materials. *Materials.* **2020**, *13*, 1–24. DOI: 10.3390/ma13214994
5. Halonen, N.; Pálvölgyi, P. S.; Bassani, A.; Fiorentini, C.; Nair, R.; Spigno, G.; Kordas, K. Bio-Based Smart Materials for Food Packaging and Sensors – A Review. *Front. Mater.* **2020**, *7*, 1-14. DOI: 10.3389/fmats.2020.00082
6. Kuorwel, K. K.; Cran, M. J.; Orbell, J. D.; Buddhadasa, S.; Bigger, S. W. Review of mechanical properties, migration, and potential applications in active food packaging systems containing nanoclays and nanosilver. *Compr. Rev. Food Sci. Food Safe.* **2015**, *14*, 411–430. DOI: 10.1111/1541-4337.12139
7. Bassani, A.; Montes, S.; Jubete, E.; Palenzuela, J.; Sanjuan, A. P.; Spigno, G. Incorporation of waste orange peels extracts into PLA films. *Chem. Eng. Trans.* **2019**, *74*, 1063–1068. DOI: 10.3303/CET1974178
8. 8. Yildirim, S.; Röcker, B. Nanomaterials for Food Packaging. In *Micro and Nano Technologies, Nanomaterials for Food Packaging*, Elsevier, 2018, pp 173-202, DOI: 10.1016/B978-0-323-51271-8.00007-3

9. Han Lyn, F.; Nur Hanani, Z. A. Effect of Lemongrass (*Cymbopogon citratus*) Essential Oil on the Properties of Chitosan Films for Active Packaging, *J. Packag. Technol. Res.* **2020**, 1-12. DOI:10.1007/s41783-019-00081-w
10. Paunonen, S. Strength and barrier enhancements of cellophane and cellulose derivative films: A Review, *BioRes.* **2013**, 8(2), 3098-3121
11. Sachdeva, S; Sachdev T. R.; Sachdeva, R. Increasing fruit and vegetable consumption: Challenges and opportunities. *Indian J. Community Med.* **2013**, 38, 192-7. DOI: 10.4103/0970-0218.120146
12. Šeregelj, V.; Šovljanski, O.; Tumbas Šaponjac, V.; Vulić, J.; Četković, G.; Markov S.; Čanadanović Brunet, J. Horned Melon (*Cucumis metuliferus* E. Meyer Ex. Naudin)-Current Knowledge on Its Phytochemicals, Biological Benefits, and Potential Applications. *Process.* **2022**, 10. DOI: 10.3390/pr10010094
13. Carpena, M.; Nuñez-Estevez, B.; Soria-Lopez, A.; Garcia-Oliveira, P.; Prieto, M. A. Essential Oils and Their Application on Active Packaging Systems: A Review. *Resources.* **2021**, 10, 7. DOI: 10.3390/resources10010007  
13<https://www.accessdata.fda.gov/scripts/cdrh/cfdocs/cfcr/CFRSearch.cfm?CFRPart=182&showFR=1>
14. Rosa, D. S.; Guedes, C. G. F.; Bardi M. A. G. Evaluation of thermal, mechanical and morphological properties of PCL/CA and PCL/CA/PE-g-GMA blends, *Polym. Test.* **2007**, 26(2), 209-215. DOI: 10.1016/j.polymertesting.2006.10.003
15. El-Naggar, M. E.; Hasanin, M.; Hashem, A. H. Eco-Friendly Synthesis of Superhydrophobic Antimicrobial Film Based on Cellulose Acetate/Polycaprolactone Loaded with the Green Biosynthesized Copper Nanoparticles for Food Packaging Application. *J. Polym. Environ.* **2021**, DOI: 10.1007/s10924-021-02318-9
16. Buchanan, C. M.; Dorschel, D.; Gardner, R. M; Komarek, R. J.; Matosky, A. J.; White, A. W.; Wood, M. D. The influence of degree of substitution on blend miscibility and biodegradation of cellulose acetate blends. *J Environ Polym Degr*, **1996**, 4, 179–195. DOI: 10.1007/BF02067452
17. Buchanan, C. M.; Buchanan, N. L.; Debenham, J. S.; Gatenholm, P.; Jacobsson, M.; Shelton, M. C.; Watterson, T. L.; Wood, M. D. Preparation and characterization of arabinoxylan esters and arabinoxylan ester/cellulose ester polymer blends. *Carbohydr. Polym.* **2003**, 52, 345-357. DOI:10.1016/S0144-8617(02)00290-4



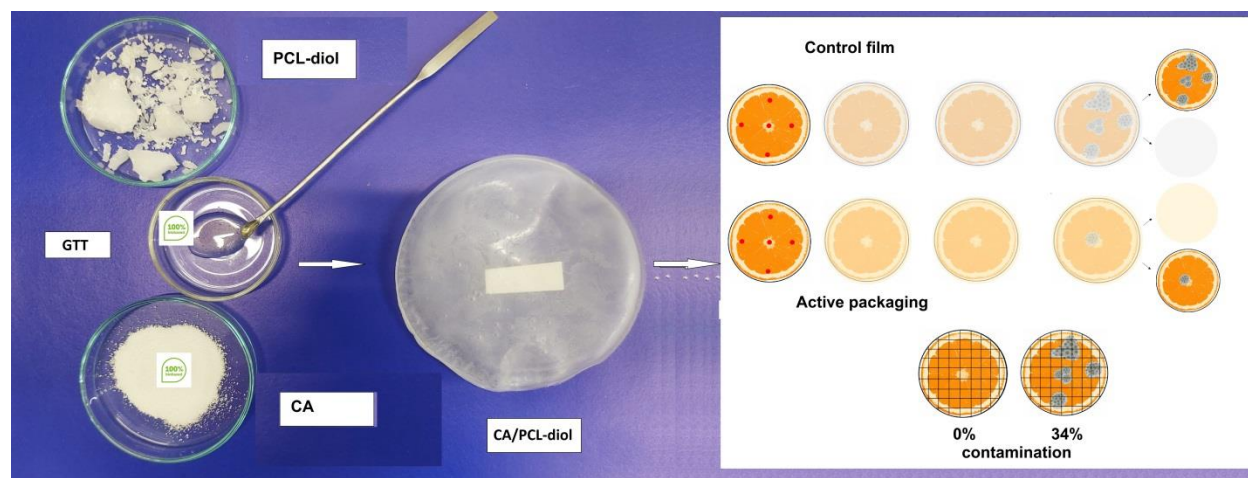
18. Miyashita, Y.; Suzuki, T.; Nishio, Y. Miscibility of cellulose acetate with vinyl polymers. *Cellulose*, **2002**, *9*, 215-223. DOI: 10.1023/A:1021144827845
19. Ohno, T.; Nishio, Y. Molecular orientation and optical anisotropy in drawn films of miscible blends composed of cellulose acetate and poly(N-vinylpyrrolidone-co-methyl methacrylate). *Macromolecules*, **2007**, *40*, 3468-3476. DOI: 10.1021/ma062920t
20. Cerqueira, D. A.; Valente, A. J. M.; Filho, G. R.; Burrows, H. D. Synthesis and properties of polyaniline–cellulose acetate blends: The use of sugarcane bagasse waste and the effect of the substitution degree. *Carbohydr. Polym.* **2009**, *78*, 402-408. DOI: 10.1016/j.carbpol.2009.04.016
21. Quintana, R.; Persenaire, O.; Lemmouchi, Y.; Sampson, J.; Martin, S.; Bonnaud, L.; Dubois, P. Enhancement of cellulose acetate degradation under accelerated weathering by plasticization with ecofriendly plasticizers. *Polym. Degrad. Stab.* **2013**, *98(9)*, 1556-1562. DOI: 10.1016/j.polymdegradstab.2013.06.032
22. Meier, M. M.; Kanis, L. A.; De Lima, J. C.; Pires, A. T. N. Poly(caprolactone triol) as plasticizer agent for cellulose acetate films: influence of the preparation procedure and plasticizer content on the physico-chemical properties. *Polym. Adv. Technol.* **2004**, *15*, 593-600. DOI: 10.1002/pat.517
23. Brügger, B.P., Martínez, L.C., Plata-Rueda, A. et al. Bioactivity of the *Cymbopogon citratus* (Poaceae) essential oil and its terpenoid constituents on the predatory bug, *Podisus nigrispinus* (Heteroptera: Pentatomidae). *Sci Rep.* **2019**, *9*, 8358 DOI:10.1038/s41598-019-44709-y
24. International Organisation for Standardisation. *Plastics — Film and sheeting — Measurement of water-contact angle of corona-treated films*; ISO 15989, Switzerland, 2004.
25. Owens, D. K.; Wendt, R. C. Estimation of the surface free energy of polymers. *J. Appl. Polym. Sci.* **1969**, *13*, 1741–1747. DOI: 10.1002/app.1969.070130815
26. Rhim, J. W.; Gennadios, A.; Weller, C. L.; Cezeirat, C.; Hanna, M. A. Soy protein isolate-dialdehyde starch films. *Ind. Crops. Prod.* **1998**, *8*, 195–203. DOI: 10.1016/S0926-6690(98)00003-X
27. International Organisation for Standardisation. *Sheet materials - Determination of water vapour transmission rate - Gravimetric (dish) method*; ISO 2528; Switzerland, 1995.
28. Rabiej, S. A. Comparison of two X-ray diffraction procedures for crystallinity determination. *Eur. Polym. J.* **1991**, *27(9)*, 947–954. DOI: 10.1016/0014-3057(91)90038-P

- 29.** Halasa, A. F.; Wathen, G. D.; Hsu, W.; Matrana, A.; Mssie, J. M. Relationship between interchain spacing of amorphous polymers and blend miscibility as determined by wide-angle X-ray scattering. *J. Appl. Polym. Sci.* **1991**, *43*, 183–190. DOI: 10.1002/app.1991.070430115
- 30.** Riabov, P.; Micić, D.; Božović, R.; Jovanović, D.; Tomić, A.; Šovljanski, O.; Filip, S.; Tosti, T.; Ostojić, S.; Blagojević, S.; Đurović, S. The chemical, biological and thermal characteristics and gastronomical perspectives of *Laurus nobilis* essential oil from different geographical origin, *Ind. Crops Prod.* **2020**, *151*, 112498. DOI: 10.1016/j.indcrop.2020.112498
- 31.** Micić, D.; Đurović, S.; Riabov, P.; Tomić, A.; Šovljanski, O.; Filip, S.; Tosti, T.; Dojčinović, B.; Božović, R.; Jovanović, D.; Blagojević, S. Rosemary Essential Oils as a Promising Source of Bioactive Compounds: Chemical Composition, Thermal Properties, Biological Activity, and Gastronomical Perspectives. *Foods.* **2021**, *10*, 2734. DOI: 10.3390/foods10112734
- 32.** Acimović, M.; Šeregelj, V.; Šovljanski, O.; Tumbas Šaponjac, V.; Švarc Gajić, J.; Brezo Borjan, T.; Pezo, L. In vitro antioxidant, antihyperglycemic, anti-inflammatory, and antimicrobial activity of *Satureja kitaibelii* Wierzb. ex Heuff. subcritical water extract, *Ind. Crops Prod.* **2021**, *169*, 113672. DOI: 10.1016/j.indcrop.2021.113672
- 33.** Liu, Z. Q.; Cunha, A. M.; Yi, X.-S.; Bernardo, C. A. Thermal Characterizations of Wood Flour/Starch Cellulose Acetate Compounds. *J. Macromol. Sci., Part B: Phys.* **2001**, *40*, 529–538. DOI: 10.1081/MB-100106175
- 34.** Pola, C. C.; Medeiros, E. A. A.; Pereira, O. L.; Souza, V. G. L.; Otoni, C. G.; Camilloto, G. P.; Soares, N. F. F. Cellulose acetate active films incorporated with oregano (*Origanum vulgare*) essential oil and organophilic montmorillonite clay control the growth of phytopathogenic fungi. *Food Packag. Shelf Life*, **2016**, *9*, 69–78. DOI: 10.1016/j.fpsl.2016.07.001
- 35.** Jamshidian, M.; Arab Tehrany, E.; Cleymand, F.; Leconte, S.; Falher, T.; Desobry, S. Effects of synthetic phenolic antioxidants on physical, structural, mechanical and barrier properties of poly lactic acid film, *Carbohydr. Polym.* **2012**, *87*, 1763-1773. DOI: 10.1016/j.carbpol.2011.09.089
- 36.** Berthet, M. A.; Angellier-Coussy, H.; Chea, V.; Guillard, V.; Gastaldi, E.; Gontard, N. Sustainable food packaging: Valorising wheat straw fibres for tuning PHBV-based composites properties. *Composites Part A-Appl. Sci. Manuf.* **2015**, *72*, 139–147. DOI: 10.1016/j.compositesa.2015.02.006

37. Kavvoosi, G.; Rahmatollahi, A.; Dadfar, S. M. M.; Purfard, A. M. Effects of essential oil on the water binding capacity, physico-mechanical properties, antioxidant and antibacterial activity of gelatin films. *LWT-Food Sci. Technol.* **2014**, *57*, 556–561. DOI: 10.1016/j.lwt.2014.02.008
38. Erceg, T.; Stupar, A.; Cvetinov, M.; Vasić, V.; Ristić, I. Investigation the correlation between chemical structure and swelling, thermal and flocculation properties of carboxymethylcellulose hydrogels. *J. Appl. Polym. Sci.* **2020**, *138(10)*, 50240. DOI: 10.1002/app.50240
39. Persenaire, O.; Alexandre, M.; Dege´e, P.; Dubois, P. Mechanisms and Kinetics of Thermal Degradation of Poly( $\epsilon$ -caprolactone). *Biomacromolecules.* **2001**, *2*, 288–294. DOI: 10.1021/bm0056310
40. Stefanović, I.; Džunuzović, J.; Džunuzović, E.; Dapčević, A.; Šešlija, S.; Balanč, B.; Dobrzyńska-Mizera, M. Composition-property relationship of polyurethane networks based on polycaprolactone diol. *Polym. Bull.* **2021**, *78*, 7103–7128. DOI: 10.1007/s00289-020-03473-0
41. Martins, P.; Sbaite, P.; Benites, C.; Maciel, M. Thermal Characterization of Orange, Lemongrass, and Basil Essential Oils. *Chem. Eng. Trans.* **2011**, *24*, 463–468. DOI: 10.3303/CET1124078
42. Lado, J.; Rodrigo, M.H.; Zacarías, L. Maturity indicators and citrus fruit quality. *Stewart Postharvest Review.* **2014**, *10*. [https://www.researchgate.net/profile/Lorenzo-Zacarias/publication/265858476\\_Maturity\\_indicators\\_and\\_citrus\\_fruit\\_quality/links/5747f02308ae14040e28d94c/Maturity-indicators-and-citrus-fruit-quality.pdf?origin=publication\\_detail](https://www.researchgate.net/profile/Lorenzo-Zacarias/publication/265858476_Maturity_indicators_and_citrus_fruit_quality/links/5747f02308ae14040e28d94c/Maturity-indicators-and-citrus-fruit-quality.pdf?origin=publication_detail)
43. Liaquat, F.; Arif, S.; Ashraf, M.; Chaudhary, H. J.; Munis, M.F.H.; Farooq, A.B.U. *Aspergillus niger* Causes Fruit Rot of Lemon and Grapefruit in Pakistan. *APS Publications* **2016**, *100*. <https://doi.org/10.1094/PDIS-02-16-0199-PDN>

## Table of content

Biodegradable active packaging films based on cellulose acetate and poly(caprolactone diol) blend with novel *green* plasticizer and incorporated lemongrass oil were developed.



## Supporting information

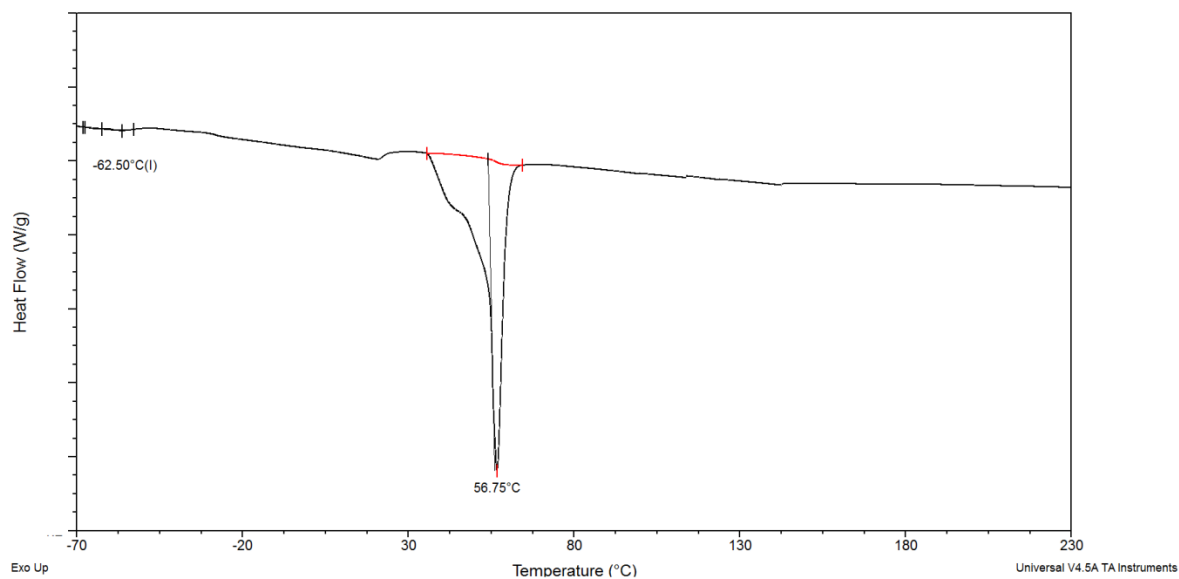


**Figure S1.** DSC curve of PCL – diol.

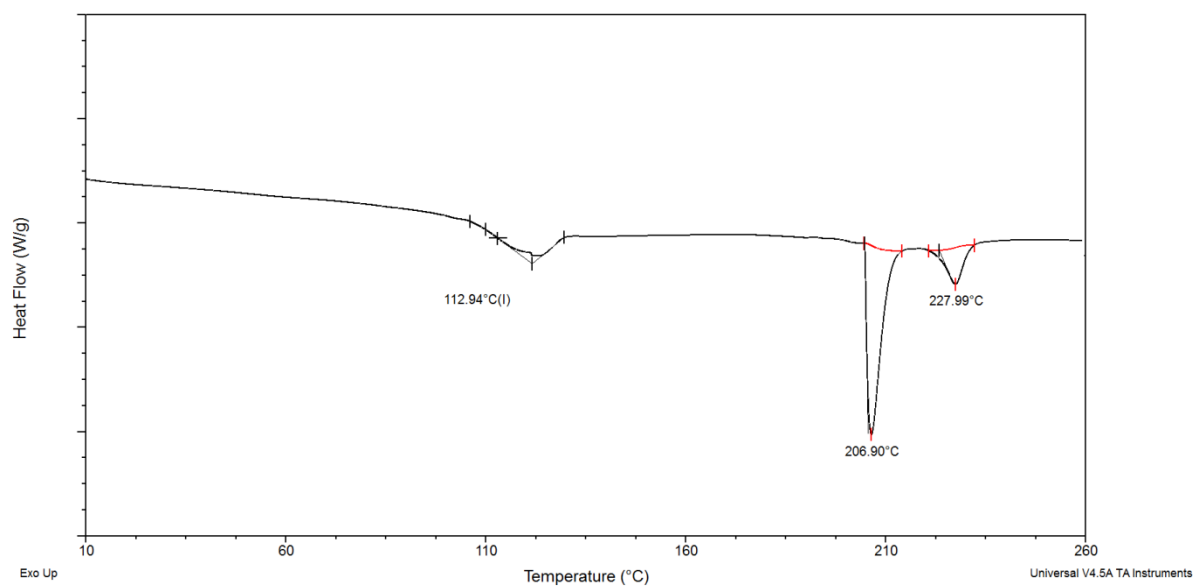


**Figure S2.** DSC curve of CA.

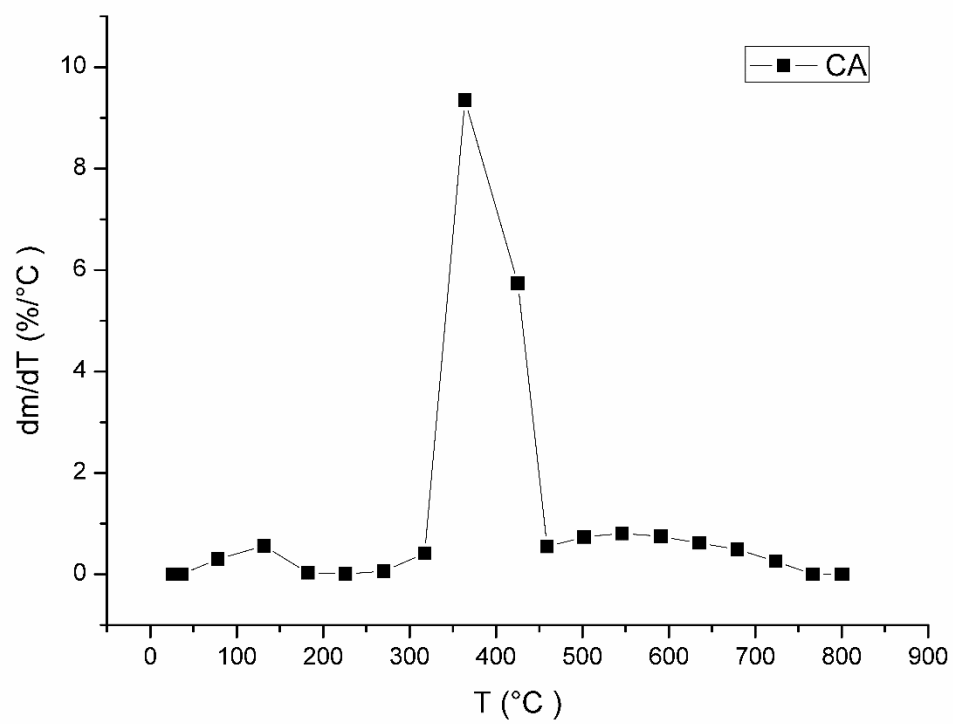


**Figure S3.** DTG curve of a neat cellulose acetate (CA).

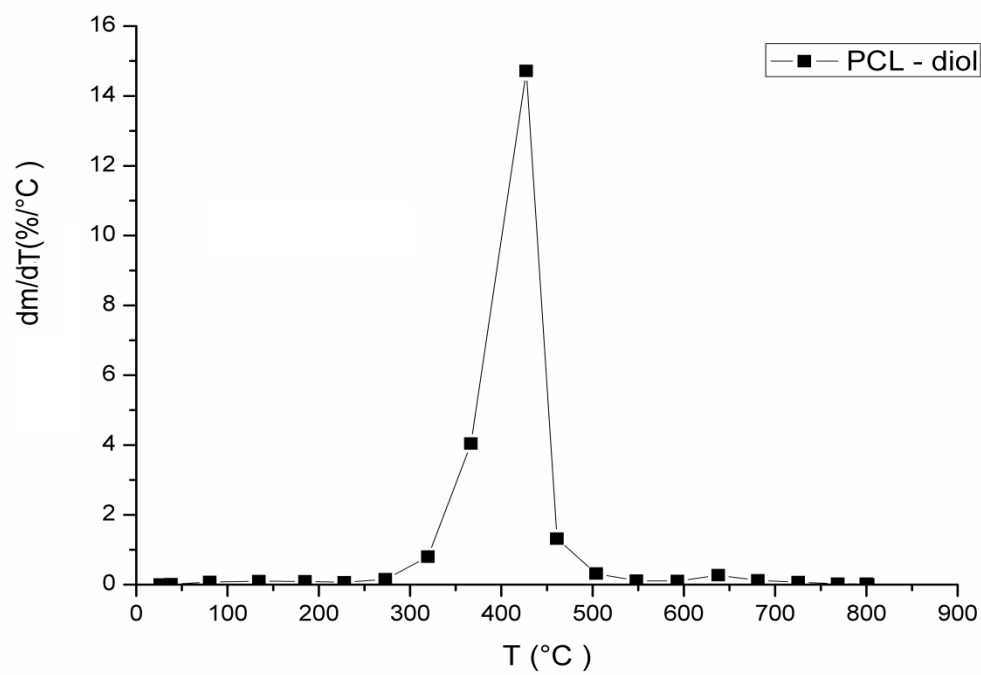


**Figure S4.** DTG curve of a neat PCL – diol.

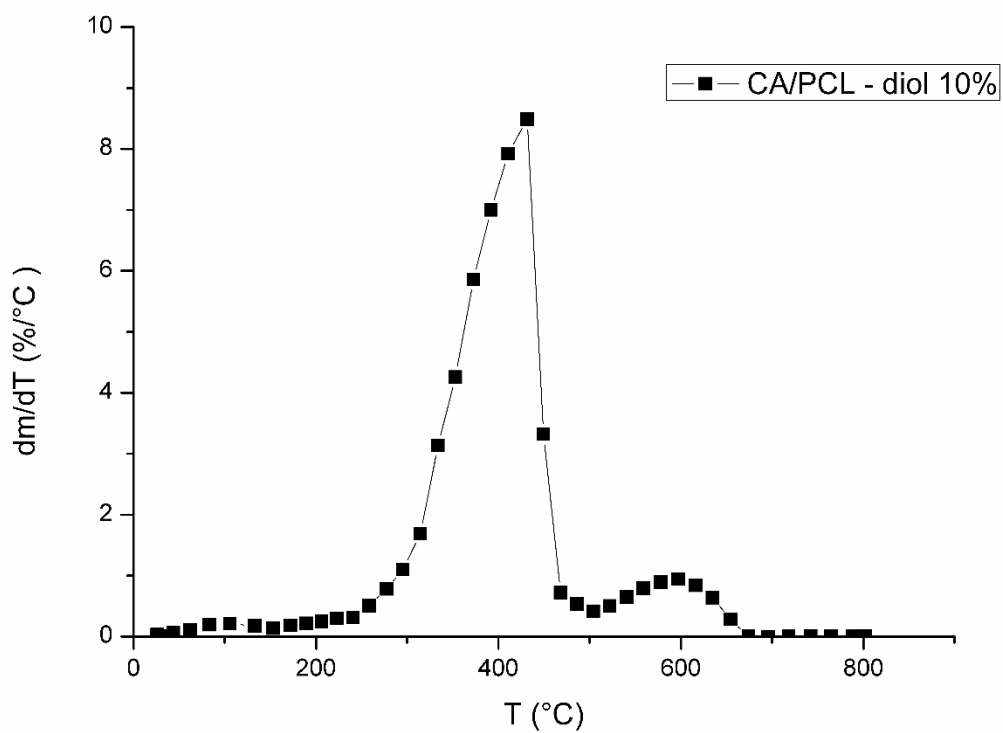


**Figure S5.** DTG of belnd CA/PCL-diol 10%.

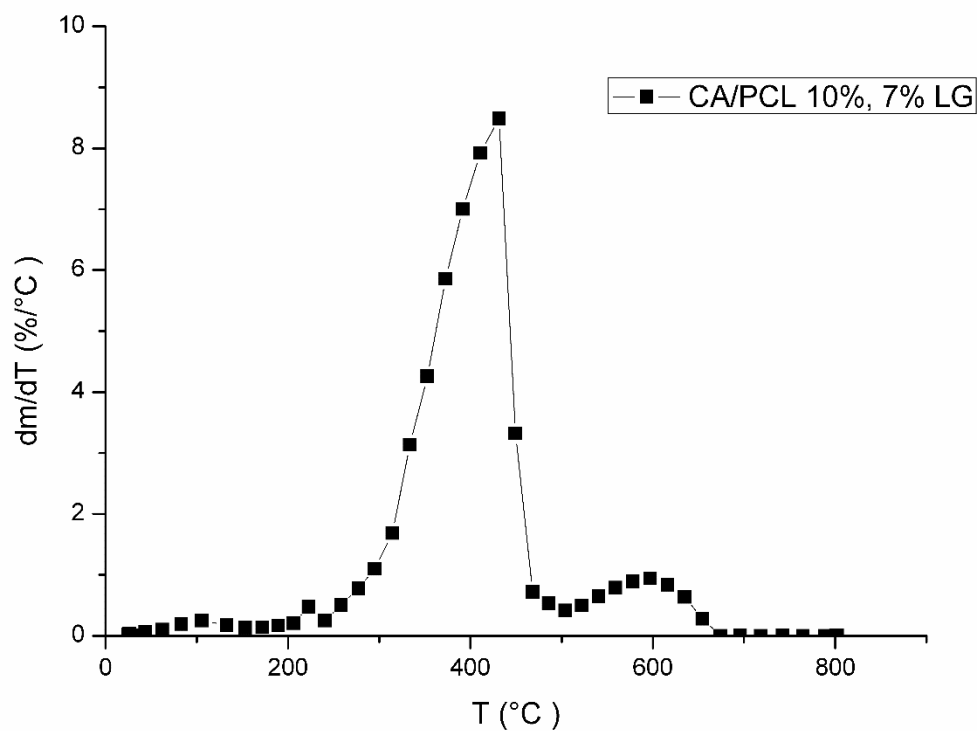


**Figure S6.** DTG of belnd CA/PCL-diol 10%, 7% LG.

## Verification

Figure 1, Figure 2, Figure 3, Figure 4, Figure 5, Figure 6, Figure 7, Figure 8, Figure 9, Figure 10, Figure 11, Figure 12, Figure 13, Figure 14, Figure S1, S2, S3 and S4 were created by the authors of manuscript and original.

All images in the TOC graphic were created by authors of manuscript and original.



